Applied Energy 155 (2015) 613–628

Contents lists available at ScienceDirect

Applied Energy

journal homepage: www.elsevier.com/locate/apenergy

# A procedure to calculate the *I–V* characteristics of thin-film photovoltaic modules using an explicit rational form

Rosario Miceli, Aldo Orioli *, Alessandra Di Gangi

*DEIM Dipartimento di Energia, Ingegneria dell'Informazione e Modelli Matematici, Università degli Studi di Palermo, Viale delle Scienze Edificio 9, 90128 Palermo, Italy*

## HIGHLIGHTS

- A new model based on a simple rational function is presented.
- The model is able to describe the *I–V* curves of thin-film photovoltaic modules.
- The derivatives in the short circuit and open circuit points were considered.
- A comparison with the Ishaque et al. and the Gupta et al. models was made.

## ARTICLE INFO

*Article history:*
Received 21 October 2014
Received in revised form 4 June 2015
Accepted 17 June 2015

*Keywords:*
Thin-film photovoltaic modules
Five-parameter model
*I–V* characteristics
Solar energy

## ABSTRACT

Accurate models of the electrical behaviour of photovoltaic modules are effective tools for system design. One or two diode equivalent circuits have been widely used even though some mathematical difficulties were found dealing with implicit equations. In this paper, a new model based on a simple rational function, which does not contain any implicit exponential form, is presented. The model was conceived in order to be used with thin-film photovoltaic modules, whose current–voltage curves are characterised by very smooth shapes. The parameters of the model are evaluated by means of the derivatives of the issued characteristics in the short circuit and open circuit points at standard rating conditions, and assuming that the calculated current–voltage curve contains the rated maximum power point of the simulated panel.

The capability of the model to calculate the current–voltage characteristic for values of the solar irradiance and cell temperature far from the standard rating conditions was verified for various thin-film technologies, such as CIS, CIGS, amorphous silicon, tandem and triple-junctions photovoltaic modules. A comparison with the results obtained by another rational model and other two-diode models, which were used to simulate the electrical behaviour of thin-film photovoltaic modules, is also presented.



## 1. Introduction

During the last years the international market of thin-film photovoltaic (PV) modules has been increasing considerably mainly due to their simple and low-cost manufacturing process. The various thin-film technologies reduce the amount of light absorbing material that is necessary to produce a solar cell. Moreover, thin-film PV panels, which employ lightweight, flexible substrates, are more resistant than crystalline PV modules and very suited to advanced applications such as building-integrated photovoltaics, curtain walls, canopies, acoustic barriers, watercrafts, vehicles and portable electronics. Because thin-film cell materials generally show reduced energy efficiencies as compared to crystalline silicon cells, the accurate modelling of PV modules is of primary concern in order to allow the designer to optimise the system performance and maximise the cost effectiveness of the system.

The simulation of the behaviour of PV modules has been conveniently done by means of nonlinear lumped-parameter equivalent circuits (one and two diode models) whose parameters were determined from experimental current–voltage (*I–V*) characteristics by means of analytical or numerical extraction techniques. The two-diode model requires the determination of seven parameters, which variously affect the shape of the *I–V* characteristic. The solution of the seven-parameter equivalent circuit, which is a complex problem, was faced assuming some analytical simplifications. Many authors propose numerical and analytical procedures to calculate the five parameters of the one-diode model. Other authors study some simplified versions of the one-diode based on a set of four parameters. The problem of the identification of the

* Corresponding author. Tel.: +39 09123861905; fax: +39 091484425.
*E-mail addresses:* orioli@dream.unipa.it, aldo.orioli@unipa.it (A. Orioli).

http://dx.doi.org/10.1016/j.apenergy.2015.06.037
0306-2619/

**Nomenclature**

| | |
|---|---|
| $a_1$, $a_2$ | diode ideality factor |
| $A$, $M$, $N$ | parameters of the proposed model |
| $C_1$, $C_2$, $C_3$ | coefficients of the $V_{oc}$ correlation |
| $D_1$, $D_2$ | coefficients of the $R_{so}$ correlation |
| $G$ | solar irradiance (W/m$^2$) |
| $G_{ref}$ | solar irradiance at SRC (1000 W/m$^2$) |
| $i$ | normalised current generated by the panel |
| $I$ | current generated by the panel (A) |
| $I_L$ | photocurrent (A) |
| $i_{mp}$ | normalised current in the maximum power point |
| $i_{mp,ref}$ | normalised current in the maximum power point at SRC |
| $I_{sc}$ | short circuit current of the panel (A) |
| $I_{sc,ref}$ | short circuit current of the panel at SRC (A) |
| $I_0$, $I_{01}$, $I_{02}$ | diode saturation current (A) |
| $k$ | Boltzmann constant (J/K) |
| $K_1$, $K_2$, $K_3$ | parameters of the Gupta et al. model |
| $N_s$ | number of cells connected in series |
| $p$ | parameter of the Ishaque et al. model |
| $q$ | electron charge (C) |
| $R_s$ | series resistance (Ω) |
| $r_{so}$ | normalised reciprocal of the slope of the $I$–$V$ characteristic for $V = V_{oc,ref}$ and $I = 0$ (Ω) |
| $R_{so}$ | reciprocal of slope of the $I$–$V$ characteristic for $V = V_{oc}$ and $I = 0$ (Ω) |
| $R_{so,ref}$ | reciprocal of slope of the $I$–$V$ characteristic for $V = V_{oc,ref}$ and $I = 0$ (Ω) |
| $R_{sh}$ | shunt resistance (Ω) |
| $r_{sho}$ | normalised reciprocal of the slope of the $I$–$V$ characteristic for $V = 0$ and $I = I_{sc,ref}$ (Ω) |
| $R_{sho}$ | reciprocal of the slope of the $I$–$V$ characteristic for $V = 0$ and $I = I_{sc}$ (Ω) |
| $R_{sho,ref}$ | reciprocal of the slope of the $I$–$V$ characteristic for $V = 0$ and $I = I_{sc,ref}$ (Ω) |
| $T$ | temperature of the PV cell (K) |
| $T_{ref}$ | temperature of the PV panel at SRC (25 °C – 298.15 K) |
| $v$ | normalised voltage generated by the PV panel |
| $v_{mp}$ | normalised voltage in the maximum power point |
| $v_{mp,ref}$ | normalised voltage in the maximum power point at SRC |
| $V$ | voltage generated by the PV panel (V) |
| $V_{oc}$ | open circuit voltage of the PV panel (V) |
| $V_{oc,ref}$ | open circuit voltage of the PV panel at SRC (V) |
| $V_{oc,200}$ | open circuit voltage of the $I$–$V$ characteristic at $G = 200$ W/m$^2$ and $T = T_{ref}$ (V) |
| $\alpha_G$ | ratio between the current irradiance and the irradiance at SRC |
| $m$ | diode ideality factor |
| $\alpha$ | thermal coefficient of the short circuit current (A/°C) |
| $\beta$ | thermal coefficient of the open circuit voltage (V/°C) |

parameters contained in the diode-based equivalent circuits is also tackled exploring the possibility of using alternative procedures such as the Lambert $W$-function, evolutionary algorithms, Padè approximants, genetic algorithms, cluster analysis, artificial neural networks, harmony search-based algorithms and small perturbations around the operating point. In addition to mathematical models, the numerical simulation offers advantages to the design, performance prediction and comprehension of the fundamental phenomena ruling the operation of devices, such as solar cells, and also permits to investigate the physics of their workings. In the literature of numerical simulators a choice is the wxAMPS software, which is an updated version of the one-dimensional simulation program Analysis of Microelectronic and Photonic Structures (AMPS-1D), which was initially developed by Zhu et al. [1]. wxAMPS is a powerful tool capable of representing the electrical transport and the optical behaviour of the solar cells, and also simulating the response of a solar cell.

In order to describe the electrical behaviour of thin-film PV cells and modules, different models, not based on equivalent circuits, are also proposed. Block et al. [2] developed a new modelling approach for the study of single and tandem pin-solar cells made from amorphous silicon. A one-dimension numerical solar cell simulation program was used by Lee et al. [3,4] to analyse the operation of CdTe and CIS solar cells. Gloeckler et al. [5] discussed the guidelines that should be considered assigning input parameters for numerical modelling of CIGS and CdTe solar cells. Solving a set of equations relative to electron and hole current densities, Das et al. [6] generated the $I$–$V$ characteristics of a standard triple-junction amorphous silicon solar cell among different failures scenarios (variations in the thickness of different layers of the cell), comparing them with the normal condition. Numerical simulations were used by Zeman et al. [7] to analyse and optimise the optical and electrical properties of tandem micromorph and triple-junction silicon-based solar cells. Xiao et al. [8] modelled a thin film triple junction solar cell using the APSYS simulator, which is a general-purpose 2D/3D finite element analysis and modelling software for semiconductor devices.

One-diode and two-diode models, which were originally thought to describe the behaviour of mono-crystalline and poly-crystalline silicon PV panels, are also used to model thin-film PV modules. Marten et al. [9] presented an improved equivalent circuit for amorphous silicon solar cells and modules; the model was a single exponential model with a new term taking into account the recombination losses in the intrinsic layer of the device. An accurate and fast method to calculate the efficiency and the fill factor of CIGS and CdTe thin-film solar modules was described by Burgelman and Niemegeers [10]. Stutenbaeumer and Mesfin [11] found that a two-diode equivalent module, which includes the contribution of the diffusion and the recombination currents and the parasitic effects of series and shunt resistance, can simulate the dark $I$–$V$ characteristics of crystalline, poly-crystalline and amorphous silicon solar cells. Using the one-diode model Brecl et al. [12] studied tandem solar cells consisting of two serially-connected thin-film solar cells under different weather and temperature, daily and seasonal conditions.

A four-parameter equivalent model was used by Xiao et al. [13] to simulate three PV panels made of different materials: CIS thin-film, poly-crystalline and mono-crystalline silicon. Burgelman et al. [14] presented a selection of currently available numerical simulation tools for thin-film solar cells and discussed their possibilities and limitations. The applicability of the one and two diode equivalent models for CIGS thin-film PV devices was analysed by Werner and Prorok [15] for a wide range of irradiance and module temperature values; the two-diode model seemed to give more reliable results than the most commonly used one-diode model. Werner and Zdanowicz [16] experimentally determined the values of the double diode model diffusion and recombination related components of the diode dark saturation current in a thin film CIGS solar cell Shell ST40. By means of linearized one-diode mathematical models, Ahmad et al. [17]

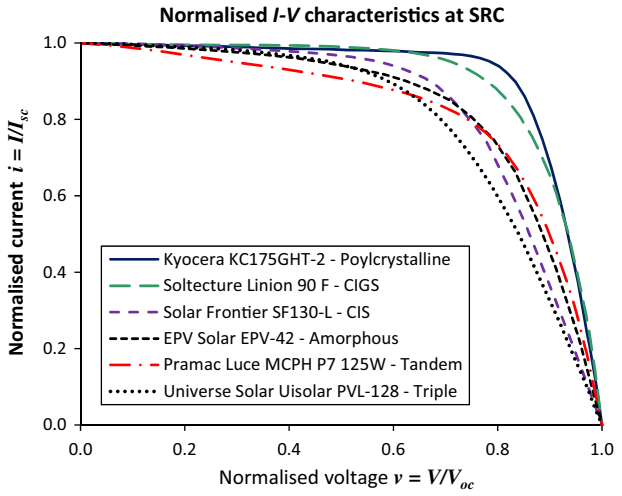


**Fig. 1.** Normalised *I–V* characteristics of crystalline and thin-film PV panels at SRC.

compared CIGS and conventional silicon cells in terms of their current–voltage characteristics, instantaneous maximum power outputs and energy conversion efficiencies.

Janssen et al. [18] proposed a model that takes into account the 2D spatial distribution of the material properties over the surface of a CIGS module; the module was described by a network of one-diode equivalent circuits that are coupled through the conductive contact layers. A one-diode model based on the differential evolution, which is a type of evolutionary algorithms, was used by Ishaque and Salam [19] to simulate the *I–V* characteristics of different types of multi-crystalline, mono-crystalline and thin-film PV panels. Molina-Garcia et al. [20] proposed to use the three-parameter Gompertz curve to describe the *I–V* characteristics of CdTe thin-film solar modules. To validate the accuracy of a new two-diode model, six PV modules of different types (multi-crystalline, mono-crystalline and thin-film) were tested by Ishaque et al. [21]; the performance of the proposed model was evaluated against the popular one-diode model.

Using MATLAB/simulink Gupta et al. [22] simulated an improved two-diode model of PV module; the accuracy of the model was validated by testing various modules of different type (multi-crystalline, mono-crystalline and thin film). Mahmoud et al. [23] proposed a parameterization approach for PV models to improve modelling accuracy and reduce implementation complexity; the effectiveness of the approach was evaluated by comparing the simulation results with the experimental data of mono-crystalline, multi-crystalline, and thin film PV modules. A model based on two subcells equivalent solar cells to predict the maximum power of a lattice matched triple junction solar cell at one sun condition for different spectra and temperatures was described by Ferdández et al. [24]. Siddique et al. [25] presented a methodology to estimate the model parameters for the five-parameter model through an optimization technique using manufacturer supplied data; the methodology was validated with five key points extracted from the *I–V* characteristics of three crystalline silicon modules and three thin film modules.

In this paper a new model, which is particularly suited to describe the electrical behaviour of thin-film PV modules, is presented. The model bases on a rational function that does not contain any implicit exponential form, which usually is the major obstacle to calculate the parameters of the one-diode equivalent model. The parameters of the proposed model can be easily extracted from the characteristics issued by manufactures using explicit relations. The capability of the model to calculate the *I–V* characteristic for values of solar irradiance and cell temperature far from the standard rating conditions (SRC) – irradiance $G_{ref} = 1000\ \mathrm{W/m^2}$, cell temperature $T_{ref} = 25\ ^\circ\mathrm{C}$ and average solar spectrum at AM 1.5 defined by IEC 60904-3 [26] – was verified for various thin-film technologies and different PV panels.

## 2. Equations for the *I–V* curves of photovoltaic panels

Different techniques are used to make crystalline and thin-film PV modules. Mono-crystalline and poly-crystalline PV cells are made of wafers sawed from silicon ingots that were obtained by means of a method of crystal growth or from molten silicon, which was carefully cooled and solidified. The material of thin-film PV modules is deposited onto a substrate or onto previously deposited layers, by means of various chemical and/or physical processes. Crystalline and thin-film PV modules show different electrical behaviours. In Fig. 1 the *I–V* characteristics at SRC of various types of PV modules are depicted; in order to better appreciate the differences between the PV typologies, the normalised values of current $i$ and voltage $v$ are used:

$$i = \frac{I}{I_{sc,ref}} \qquad v = \frac{V}{V_{oc,ref}} \tag{1}$$

where $I_{sc,ref}$ and $V_{oc,ref}$ are the short circuit current and the open circuit voltage of the PV panel at SRC, respectively.

Crystalline PV panels, like Kyocera KC175GHT-2, show a curve whose "knee" is close to the maximum power point (1,1) of the normalised *I–V* curve of the ideal PV device; conversely, thin-film PV panels are generally characterised by smoother curves. Thin-film modules tend to have values of the fill factor (FF) that are smaller than the values of the PV panels based on the use of crystalline silicon wafers. Even the values of the derivatives of the *I–V* curves in correspondence with the short circuit (1, 0) and

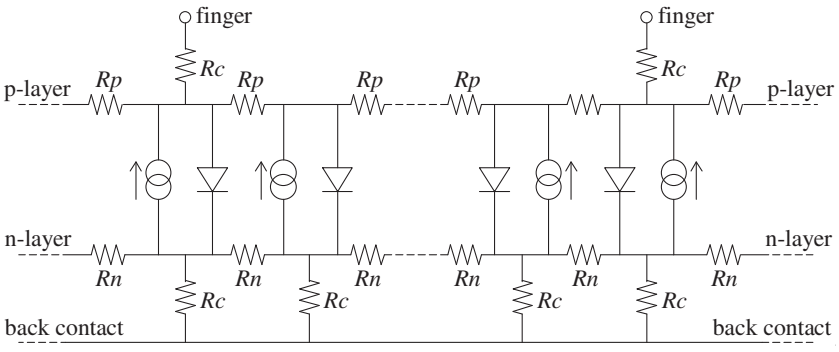


**Fig. 2.** Distributed constant equivalent circuit.

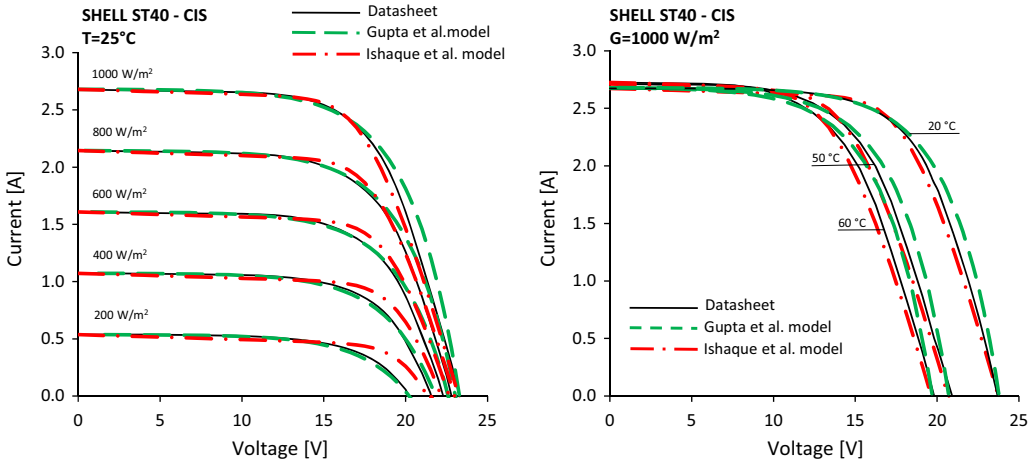


**Fig. 3.** Comparison between the measured *I–V* characteristics of Shell ST40 and the characteristics calculated with the Gupta et al. and the Ishaque et al. models.

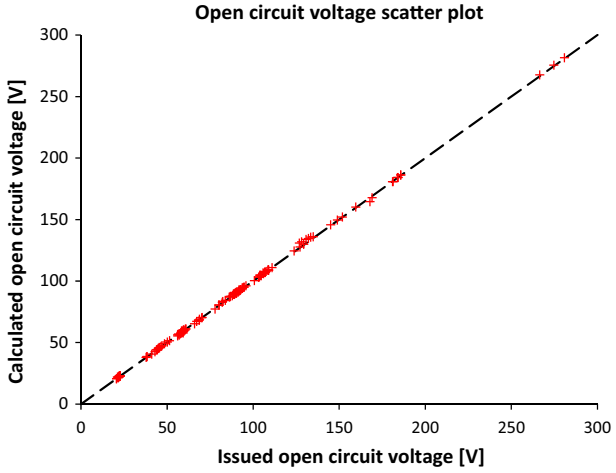


**Fig. 4.** Comparison between the values of $V_{oc}(G)$ calculated with Eq. (34) and the values extracted from the issued *I–V* characteristics at $T = 25$ °C and $G = 400$, 600 and 800 W/m$^2$.

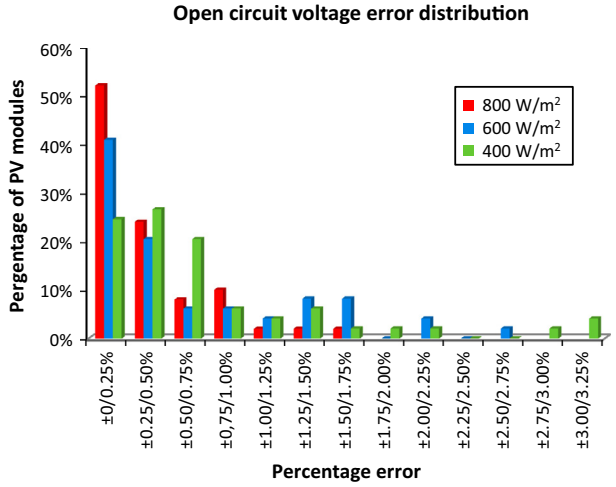


**Fig. 5.** Histogram of the percentage of panels versus the percentage error of the values of $V_{oc}$ calculated with Eq. (34).

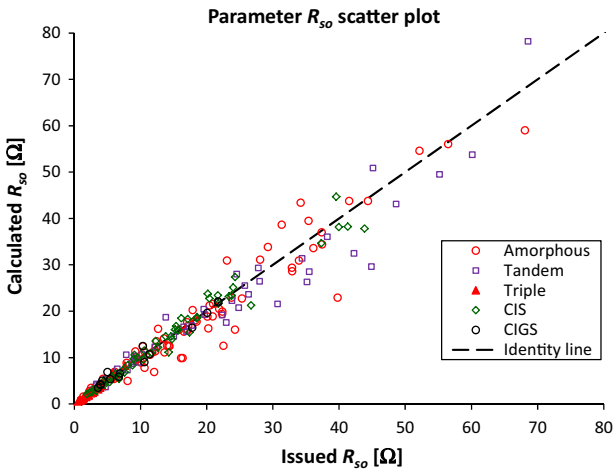


**Fig. 6.** Comparison between the values of $R_{so}(G)$ calculated with Eq. (39) and the values extracted from the issued *I–V* characteristics at $T = 25$ °C and $G = 200$, 400, 600 and 800 W/m$^2$.

open circuit (0, 1) points are different. The values of such derivatives indicate how the electrical behaviour of a PV panel is far from the *I–V* characteristics of an ideal electrical source. Because ideal current or voltage sources are not affected by internal energy dissipation, their *I–V* characteristics are straight lines parallel to the voltage axis or the current axis, respectively. Due to the internal series resistance, the right part of the *I–V* curve of a PV panel slants to the left. Analogously, for the presence of the internal shunt resistance the left part of the *I–V* characteristic may be not perfectly horizontal. In Fig. 1 the slopes of the *I–V* curves near the short circuit and open circuit points confirm the fact that the high quality silicon slabs of poly-crystalline and CIGS modules dissipate less energy than the materials used to make amorphous, tandem and triple junction PV panels. The presence of internal dissipation generally reduces both the FF and the energy efficiency of PV panels; actually, the Kyocera KC175GHT-2 and the Soltecture Linion 90 F have values of FF of 0.74 and 0.71, respectively, whereas the corresponding values of the energy efficiency at SRC are 13.7% and 10.87%. However, sometimes it may also happen that a greater value of the FF corresponds to a smaller value of the energy efficiency and vice versa: the amorphous EPV-42 has a FF of 0.60 and an efficiency of 5.3% at SRC, whereas the triple junction Uisolar PVL-128 has a FF of 0.56 and an efficiency of 5.9%.

Crystalline PV cells share with semiconductor electronic devices, such as diodes and transistors, the same processing and

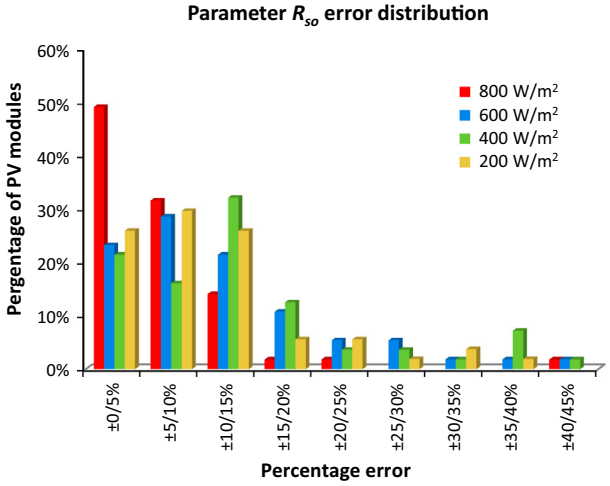


**Fig. 7.** Histogram of the percentage of panels versus the percentage error of the values of $R_{so}$ calculated with Eq. (39).

manufacturing techniques used to create p–n junctions. Because PV cells are illuminated silicon diodes, Shockley [27] described their *I–V* characteristic with the equation:

$$I = I_L - I_0\left(e^{\frac{qV}{mkT}} - 1\right) \tag{2}$$

where $I_L$ is the photocurrent generated by illumination, $I_0$ is the reverse saturation current of the diode, $q$ is the electron charge ($1.602 \cdot 10^{-19}$ C), $k$ is the Boltzmann constant ($1.381 \cdot 10^{-23}$ J/K), $T$ is the p–n junction temperature (K) and m, in compliance with the traditional theory of semiconductors, is 1 for the ideal PV cell, and it is increased as it is further from that ideal case (in [28] several calculated values of this parameter can be shown for different technologies). Wolf and Rauscenbach [29] observed that in a PV cell the photocurrent is not generated by only one diode but it is the global effect of the presence of a multitude of flanked diodes that are uniformly distributed throughout the surface that separates the two semiconductor slabs of the p–n junction. For this reason, a PV cell should be described with the equivalent electric circuit depicted in Fig. 2, which contains a multitude of different lumped elementary components, each one made up of a current generator, a diode and a series resistance.

The elementary diodes are inter-connected by resistors $R_p$ and $R_n$, which represent the transverse distributed resistances of p-layer and n-layer, respectively; resistors $R_c$ are included to consider the contact resistance between the semiconductor and the fingers, or the back contact. Because such equivalent circuit would be too complex to be used, simplified equivalent circuits, containing only one or two diode, a current generator and two resistors, $R_s$ and $R_{sh}$, were proposed. The one-diode and two-diode equivalent circuits of a PV cell were also used to describe the electrical behaviour of solar modules, as they are composed of PV cells connected

**Table 2**
Evaluated model parameters at SRC.

| Panel | Type | $r_{so,min}$ | $r_{so}$ | $A$ | $M$ | $N$ |
|---|---|---|---|---|---|---|
| Soltecture Linion 90 F | CIGS | 0.002 | 0.102 | 0.024 | 19.926 | 9.941 |
| Solar Frontier SF130-L | CIS | 0.003 | 0.269 | 0.031 | 7.544 | 8.261 |
| EPV Solar EPV-42 | Amorphous | 0.010 | 0.195 | 0.077 | 10.654 | 6.934 |
| Pramac Luce MCPH P7 125 W | Tandem | 0.026 | 0.160 | 0.162 | 13.479 | 7.691 |
| Universe Solar Uisolar PVL-128 | Triple | 0.005 | 0.301 | 0.054 | 6.826 | 5.922 |

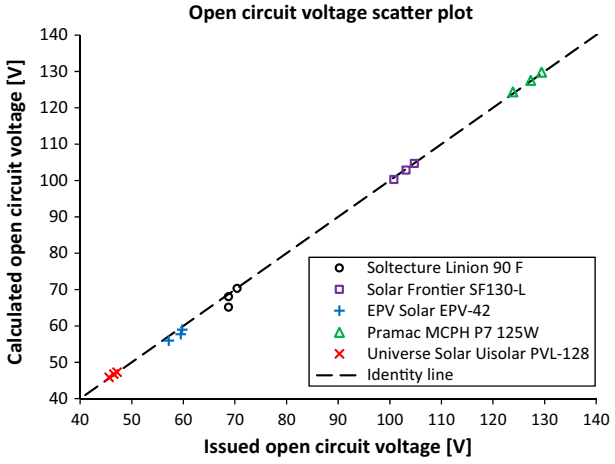


**Fig. 8.** Comparison between the values of $V_{oc}(G)$ calculated with Eq. (34) and the values extracted from the issued *I–V* characteristics at $T = 25$ °C and $G = 400$, 600 and 800 W/m$^2$.

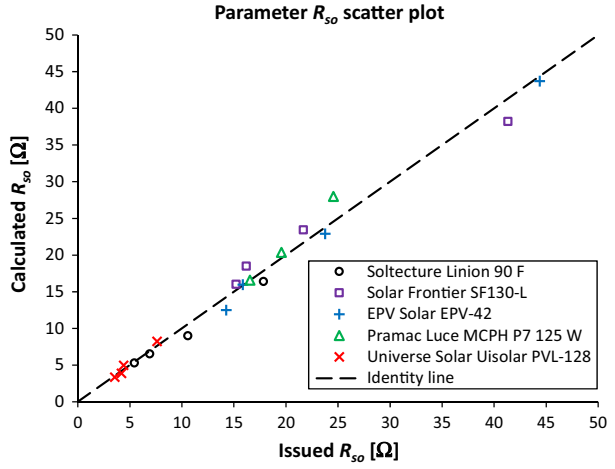


**Fig. 9.** Comparison between the values of $R_{so}(G)$ calculated with Eq. (39) and the values extracted from the issued *I–V* characteristics at $T = 25$ °C and $G = 200$, 400, 600 and 800 W/m$^2$.

**Table 1**
Data for the evaluation of the proposed model parameters.

| Panel | Type | $V_{oc}$ (V) | $I_{sc}$ (A) | $V_{mp}$ (V) | $I_{mp}$ (A) | $V_{oc,200}$ (V) | $R_{so}$ (Ω) | $R_{sho}$ (Ω) | $\beta$ (V/°C) | $\alpha$ (A/°C) |
|---|---|---|---|---|---|---|---|---|---|---|
| Soltecture Linion 90 F | CIGS | 72.20 | 1.80 | 57.50 | 1.59 | 61.00 | 4.07 | 1704.5 | $-2.64 \cdot 10^{-1}$ | $1.74 \cdot 10^{-4}$ |
| Solar Frontier SF130-L | CIS | 106.00 | 2.10 | 75.00 | 1.80 | 96.10 | 13.59 | 1640.7 | $-3.20 \cdot 10^{-1}$ | $2.09 \cdot 10^{-4}$ |
| EPV Solar EPV-42 | Amorphous | 60.00 | 1.18 | 42.50 | 1.00 | 57.20 | 9.91 | 660.8 | $-2.80 \cdot 10^{-3}$ | $9.00 \cdot 10^{-4}$ |
| Pramac Luce MCPH P7 125W | Tandem | 131.40 | 1.54 | 100.00 | 1.21 | 118.60 | 13.69 | 526.3 | $-4.05 \cdot 10^{-2}$ | $1.09 \cdot 10^{-3}$ |
| Universe Solar Uisolar PVL-128 | Triple | 47.60 | 4.80 | 32.50 | 3.90 | 43.90 | 2.98 | 182.8 | $-3.80 \cdot 10^{-3}$ | $1.00 \cdot 10^{-3}$ |

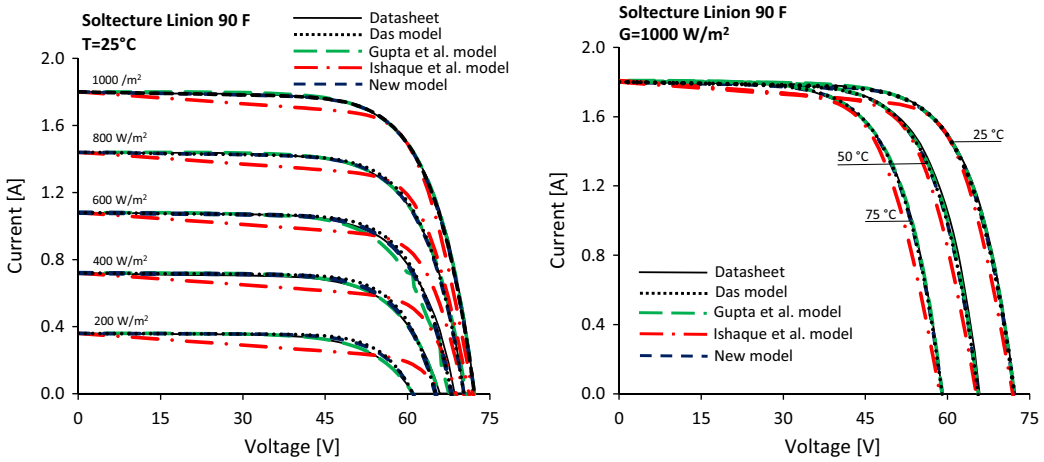


**Fig. 10.** Comparison between the issued *I–V* characteristics of Soltecture Linion 90 F (CIGS) and the characteristics calculated with the Das, the Gupta et al., the Ishaque et al. and the proposed models.

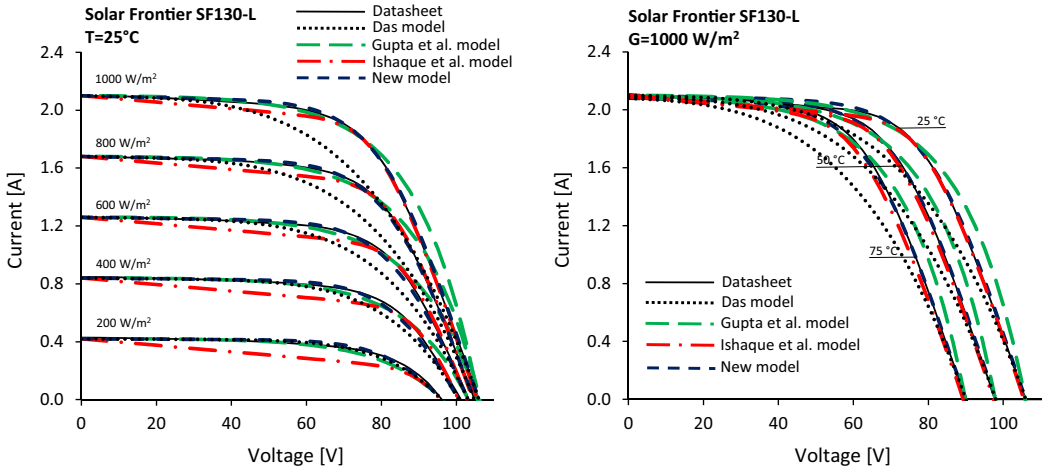


**Fig. 11.** Comparison between the issued *I–V* characteristics of Solar Frontier SF130-L (CIS) and the characteristics calculated with the Das, the Gupta et al., the Ishaque et al. and the proposed models.

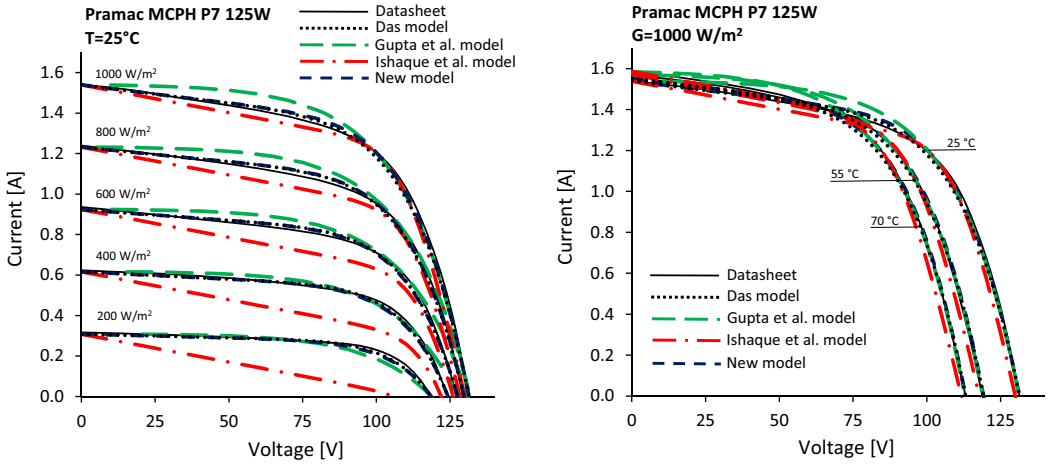


**Fig. 12.** Comparison between the issued *I–V* characteristics of Pramac Luce MCPH P7 125 W (Tandem) and the characteristics calculated with the Das, the Gupta et al., the Ishaque et al. and the proposed models.

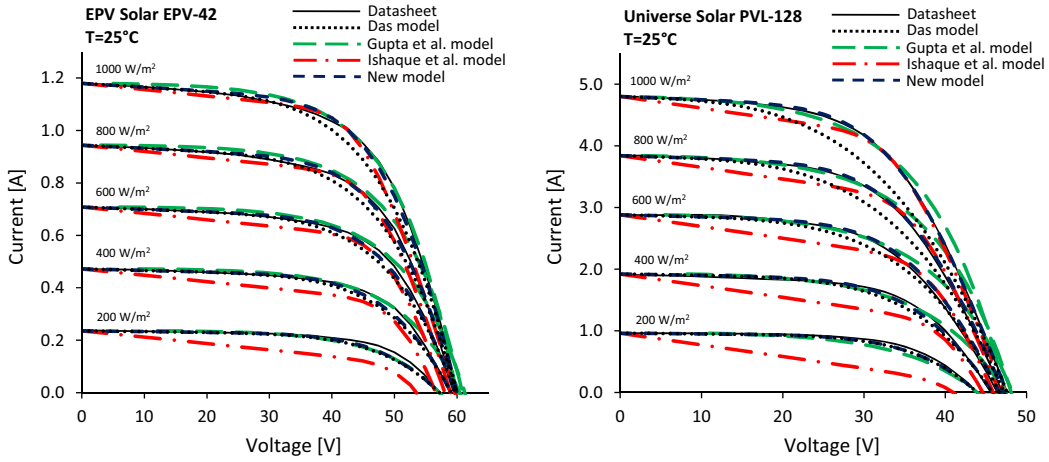


**Fig. 13.** Comparison between the issued *I–V* characteristics of EPV Solar EPV-42 (Amorphous) and Universe Solar Uisolar PVL-128 (Triple junction), and the characteristics calculated with the Das, the Gupta et al., the Ishaque et al. and the proposed models.

**Table 3**
Maximum current differences between the issued and the calculated *I–V* characteristics at temperature $T = 25$ °C.

| Parameters at the maximum difference points | | | Irradiance (W/m$^2$) | | | | |
|---|---|---|---|---|---|---|---|
| | | | 200 | 400 | 600 | 800 | 1000 |
| Soltecture Linion 90 F | Proposed model | Voltage (V) | 53.8 | 65.0 | 67.5 | 67.5 | 70.0 |
| | | Issued Current (A) | 0.234 | 0.094 | 0.182 | 0.512 | 0.519 |
| | | Calculated Current (A) | 0.262 | 0.017 | 0.085 | 0.486 | 0.471 |
| | | Difference (A) | 0.028 | −0.077 | **−0.097** | −0.026 | −0.048 |
| | Das model | Voltage (V) | 53.8 | 65.0 | 67.5 | 70.0 | 70.0 |
| | | Issued Current (A) | 0.234 | 0.094 | 0.182 | 0.085 | 0.519 |
| | | Calculated Current (A) | 0.274 | 0.017 | 0.085 | 0.061 | 0.472 |
| | | Difference (A) | 0.040 | −0.077 | **−0.097** | −0.024 | −0.047 |
| | Ishaque et al. model | Voltage (V) | 61.0 | 65.9 | 68.6 | 70.4 | 70.0 |
| | | Issued Current (A) | 0.000 | 0.000 | 0.000 | 0.000 | 0.519 |
| | | Calculated Current (A) | 0.174 | 0.283 | 0.232 | 0.134 | 0.340 |
| | | Difference (A) | 0.174 | **0.283** | 0.232 | 0.134 | −0.179 |
| | Gupta et al. model | Voltage (V) | 24.9 | 64.9 | 65.9 | 70.4 | 70.4 |
| | | Issued Current (A) | 0.354 | 0.099 | 0.382 | 0.005 | 0.442 |
| | | Calculated Current (A) | 0.358 | 0.086 | 0.357 | 0.053 | 0.413 |
| | | Difference (A) | 0.004 | 0.013 | −0.025 | **0.048** | −0.029 |
| Solar Frontier SF130-L | Proposed model | Voltage (V) | 62.5 | 87.5 | 85.0 | 82.5 | 92.5 |
| | | Issued Current (A) | 0.377 | 0.532 | 0.903 | 1.276 | 0.966 |
| | | Calculated Current (A) | 0.400 | 0.494 | 0.866 | 1.253 | 0.998 |
| | | Difference (A) | 0.023 | **−0.038** | −0.037 | −0.023 | 0.032 |
| | Das model | Voltage (V) | 87.5 | 82.5 | 82.5 | 80.0 | 77.5 |
| | | Issued Current (A) | 0.216 | 0.645 | 0.975 | 1.354 | 1.733 |
| | | Calculated Current (A) | 0.189 | 0.552 | 0.815 | 1.126 | 1.435 |
| | | Difference (A) | −0.027 | −0.093 | −0.160 | −0.228 | **−0.298** |
| | Ishaque et al. model | Voltage (V) | 65.0 | 60.0 | 60.0 | 50.0 | 50.0 |
| | | Issued Current (A) | 0.372 | 0.796 | 1.203 | 1.634 | 2.039 |
| | | Calculated Current (A) | 0.274 | 0.705 | 1.125 | 1.568 | 1.987 |
| | | Difference (A) | **−0.098** | −0.091 | −0.078 | −0.066 | −0.052 |
| | Gupta et al. model | Voltage (V) | 85.7 | 99.3 | 100.4 | 98.9 | 96.1 |
| | | Issued Current (A) | 0.242 | 0.086 | 0.176 | 0.397 | 0.715 |
| | | Calculated Current (A) | 0.204 | 0.183 | 0.358 | 0.624 | 0.966 |
| | | Difference (A) | −0.038 | 0.097 | 0.182 | 0.227 | **0.251** |
| EPV Solar EPV-42 | Proposed model | Voltage (V) | 50.0 | 50.0 | 50.0 | 58.9 | 50.0 |
| | | Issued Current (A) | 0.154 | 0.325 | 0.482 | 0.063 | 0.782 |
| | | Calculated Current (A) | 0.130 | 0.296 | 0.455 | 0.085 | 0.751 |
| | | Difference (A) | −0.024 | −0.029 | −0.027 | 0.022 | **−0.031** |
| | Das model | Voltage (V) | 50.0 | 50.0 | 50.0 | 50.0 | 50.0 |
| | | Issued Current (A) | 0.154 | 0.325 | 0.482 | 0.626 | 0.782 |
| | | Calculated Current (A) | 0.126 | 0.285 | 0.435 | 0.575 | 0.704 |
| | | Difference (A) | −0.028 | −0.040 | −0.047 | −0.051 | **−0.078** |
| | Ishaque et al. model | Voltage (V) | 52.5 | 55.0 | 57.5 | 54.7 | 54.7 |
| | | Issued Current (A) | 0.116 | 0.175 | 0.133 | 0.371 | 0.483 |
| | | Calculated Current (A) | 0.030 | 0.088 | 0.038 | 0.302 | 0.375 |
| | | Difference (A) | −0.086 | −0.087 | −0.095 | −0.069 | **−0.108** |
| | Gupta et al. model | Voltage (V) | 49.6 | 59.1 | 58.5 | 58.0 | 55.0 |

(*continued on next page*)

**Table 3** (*continued*)

| Parameters at the maximum difference points | | | Irradiance (W/m$^2$) | | | | |
|---|---|---|---|---|---|---|---|
| | | | 200 | 400 | 600 | 800 | 1000 |
| | | Issued Current (A) | 0.158 | 0.000 | 0.070 | 0.131 | 0.461 |
| | | Calculated Current (A) | 0.134 | 0.071 | 0.182 | 0.253 | 0.489 |
| | | Difference (A) | −0.024 | 0.071 | 0.112 | **0.122** | 0.028 |
| Pramac Luce MCPH P7 125W | Proposed model | Voltage (V) | 107.5 | 107.5 | 115.0 | 115.0 | 124.1 |
| | | Issued Current (A) | 0.181 | 0.410 | 0.492 | 0.686 | 0.500 |
| | | Calculated Current (A) | 0.156 | 0.382 | 0.460 | 0.659 | 0.461 |
| | | Difference (A) | −0.025 | −0.028 | −0.032 | −0.027 | **−0.039** |
| | Das model | Voltage (V) | 110.0 | 117.5 | 115.0 | 115.0 | 112.5 |
| | | Issued Current (A) | 0.156 | 0.232 | 0.492 | 0.686 | 0.965 |
| | | Calculated Current (A) | 0.134 | 0.209 | 0.462 | 0.652 | 0.913 |
| | | Difference (A) | −0.022 | −0.023 | −0.030 | −0.034 | **−0.052** |
| | Ishaque et al. model | Voltage (V) | 97.5 | 95.0 | 80.0 | 124.1 | 125.0 |
| | | Issued Current (A) | 0.241 | 0.500 | 0.804 | 0.332 | 0.450 |
| | | Calculated Current (A) | 0.035 | 0.350 | 0.703 | 0.237 | 0.307 |
| | | Difference (A) | **−0.206** | −0.150 | −0.101 | −0.095 | −0.143 |
| | Gupta et al. model | Voltage (V) | 107.9 | 122.8 | 127.7 | 129.2 | 60.0 |
| | | Issued Current (A) | 0.177 | 0.055 | 0.000 | 0.015 | 1.413 |
| | | Calculated Current (A) | 0.127 | 0.133 | 0.137 | 0.146 | 1.494 |
| | | Difference (A) | −0.050 | 0.078 | **0.137** | 0.131 | 0.081 |
| Universe Solar Uisolar PVL-128 | Proposed model | Voltage (V) | 35.0 | 37.5 | 41.3 | 42.5 | 22.5 |
| | | Issued Current (A) | 0.745 | 1.291 | 1.134 | 1.269 | 4.570 |
| | | Calculated Current (A) | 0.684 | 1.226 | 1.236 | 1.340 | 4.599 |
| | | Difference (A) | −0.061 | −0.065 | **0.102** | 0.071 | 0.029 |
| | Das model | Voltage (V) | 35.0 | 35.0 | 31.3 | 33.8 | 32.5 |
| | | Issued Current (A) | 0.745 | 1.496 | 2.442 | 2.992 | 3.895 |
| | | Calculated Current (A) | 0.681 | 1.376 | 2.312 | 2.706 | 3.413 |
| | | Difference (A) | −0.064 | −0.120 | −0.130 | −0.286 | **−0.482** |
| | Ishaque et al. model | Voltage (V) | 32.5 | 30.0 | 22.5 | 22.5 | 20.0 |
| | | Issued Current (A) | 0.823 | 1.712 | 2.751 | 3.662 | 4.625 |
| | | Calculated Current (A) | 0.340 | 1.347 | 2.453 | 3.412 | 4.420 |
| | | Difference (A) | **−0.483** | −0.365 | −0.298 | −0.250 | −0.205 |
| | Gupta et al. model | Voltage (V) | 35.9 | 45.7 | 45.5 | 44.0 | 42.5 |
| | | Issued Current (A) | 0.702 | 0.000 | 0.229 | 0.880 | 1.665 |
| | | Calculated Current (A) | 0.579 | 0.328 | 0.774 | 1.418 | 2.015 |
| | | Difference (A) | −0.123 | 0.328 | **0.545** | 0.538 | 0.350 |

Bold values indicate for each model the highest value of maximum current differences between the issued and the calculated *I–V* characteristics.

in series and/or parallel. The two-diode equivalent circuit of a PV module is described by the well-known equation:

$$I = I_L - I_{01}\left(e^{\frac{V+IR_s}{a_1 V_T}} - 1\right) - I_{02}\left(e^{\frac{V+IR_s}{a_2 V_T}} - 1\right) - \frac{V + IR_s}{R_{sh}} \quad (3)$$

where following the traditional theory, the photocurrent $I_L$ depends on the solar irradiance, the diode saturation currents $I_{01}$ and $I_{02}$ are affected by the cell temperature, $a_1$ and $a_2$ are the diode ideality factors and $V_T = N_s kT/q$, in which $N_s$ is the number of cells of the panel that are connected in series. The values of $R_s$, $R_{sh}$, $I_{01}$ and $I_{02}$ variously affect the *I–V* characteristic calculated with Eq. (3). The ratio $I_{02}/I_{01}$ particularly influences the shape of the curve close to the maximum power point [30]. Actually, if $I_{02}$ is zero, a sharp "knee" is observed; by increasing the value of $I_{02}/I_{01}$ smoother curves are obtained.

Some authors used the two-diode model to simulate the electrical behaviour of thin-film PV panels. Ishaque et al. [21] calculated the *I–V* characteristics with the following equations:

$$I = I_L - I_0\left(e^{\frac{V+IR_s}{V_T}} + e^{\frac{V+IR_s}{(p-1)V_T}} - 2\right) - \frac{V + IR_s}{R_{sh}} \quad (4)$$

$$I_0 = I_{01} = I_{02} = \frac{I_{sc,ref} + \alpha(T - T_{ref})}{e^{\frac{V_{oc,ref} + \beta(T - T_{ref})}{[(a_1 + a_2)/p]V_T}} - 1} \quad (5)$$

in which $\alpha$ and $\beta$ are the thermal coefficients of the short circuit current and of the open circuit voltage, respectively. In order to reach the best match between the proposed model and the practical *I–V* curve, $a_1 = 1$, $a_2 \geqslant 1.2$ and $p \geqslant 2.2$ were set. Parameters $R_s$ and $R_{sh}$ were obtained assuming that the maximum power point calculated with the model at SRC coincided with the measured maximum power point of the simulated PV panel. To reach the maximum power point matching, the value of $R_s$ was iteratively increased while simultaneously calculating the $R_{sh}$ value.

Gupta et al. [22] proposed the following form of Eq. (3):

$$I = I_{L,ref} - I_{01}\left(e^{K_2 \frac{V}{V_{oc,ref}}} - 1\right) - K_1 I_{01}\left(e^{K_2 \frac{V}{V_{oc,ref}}} - 1\right) \quad (6)$$

which was obtained ignoring the last term of Eq. (3) and considering the following positions:

$$a_1 = a_2 = 1 \; I_{02} = K_1 I_{01} \frac{q(V + IR_s)}{kT} = \frac{V}{K_2 V_{oc,ref}} \quad (7)$$

Moreover, assuming $I_{L,ref} = I_{sc,ref}$ and $I_{01} = K_3\, I_{sc,ref}$, Eq. (6) was rewritten as:

$$I = I_{sc,ref}\left[1 - K_3\left(e^{K_2 \frac{V}{V_{oc,ref}}} - 1\right)(1 + K_1)\right] \quad (8)$$

Imposing the maximum power point and the open circuit point conditions, coefficient $K_3$ and $K_2$ were calculated from Eq. (8):

$$K_3 = \frac{1 - \frac{I_{mp,ref}}{I_{sc,ref}}}{\left(e^{K_2 \frac{V_{mp,ref}}{V_{oc,ref}}} - 1\right)(1 + K_1)} \quad K_2 = \frac{\frac{V_{mp,ref}}{V_{oc,ref}} - 1}{\ln\left(1 - \frac{I_{mp,ref}}{I_{sc,ref}}\right)} \quad (9)$$

It was assumed that $K_1 = T^{2/5}/3.77$. The effects of temperature and solar radiation were included by adding to the values of $I$ and $V$ of Eq. (8) the following corrections:

**Table 4**
Maximum current differences between the issued and the calculated *I–V* characteristics at irradiance $G = 1000\ W/m^2$.

| parameters at the maximum difference points | | | Temperature (°C) | | | | |
|---|---|---|---|---|---|---|---|
| | | | 25 | 50 | 55 | 70 | 75 |
| Soltecture Linion 90 F | Proposed model | Voltage (V) | 70.0 | 65.0 | – | – | 53.8 |
| | | Issued Current (A) | 0.519 | 0.240 | – | – | 0.977 |
| | | Calculated Current (A) | 0.471 | 0.143 | – | – | 0.943 |
| | | Difference (A) | −0.048 | **−0.097** | – | – | −0.034 |
| | Das model | Voltage (V) | 70.0 | 65.0 | – | – | 56.3 |
| | | Issued Current (A) | 0.519 | 0.240 | – | – | 0.608 |
| | | Calculated Current (A) | 0.472 | 0.143 | – | – | 0.575 |
| | | Difference (A) | −0.047 | **−0.097** | – | – | −0.033 |
| | Ishaque et al. model | Voltage (V) | 70.0 | 62.5 | – | – | 55.0 |
| | | Issued Current (A) | 0.519 | 0.723 | – | – | 0.807 |
| | | Calculated Current (A) | 0.340 | 0.475 | – | – | 0.593 |
| | | Difference (A) | −0.179 | **−0.248** | – | – | −0.214 |
| | Gupta et al. model | Voltage (V) | 70.4 | 64.7 | – | – | 38.1 |
| | | Issued Current (A) | 0.442 | 0.310 | – | – | 1.714 |
| | | Calculated Current (A) | 0.413 | 0.235 | – | – | 1.722 |
| | | Difference (A) | −0.029 | **−0.075** | – | – | 0.008 |
| Solar Frontier SF130-L | Proposed model | Voltage (V) | 92.5 | 65.0 | – | – | 60.0 |
| | | Issued Current (A) | 0.966 | 1.867 | – | – | 1.802 |
| | | Calculated Current (A) | 0.998 | 1.845 | – | – | 1.768 |
| | | Difference (A) | 0.032 | −0.022 | – | – | **−0.034** |
| | Das model | Voltage (V) | 77.5 | 70.0 | – | – | 62.5 |
| | | Issued Current (A) | 1.733 | 1.729 | – | – | 1.727 |
| | | Calculated Current (A) | 1.435 | 1.415 | – | – | 1.396 |
| | | Difference (A) | −0.298 | −0.314 | – | – | **−0.331** |
| | Ishaque et al. model | Voltage (V) | 50.0 | 35.0 | – | – | 72.5 |
| | | Issued Current (A) | 2.039 | 2.069 | – | – | 1.250 |
| | | Calculated Current (A) | 1.987 | 2.016 | – | – | 1.168 |
| | | Difference (A) | −0.052 | −0.053 | – | – | **−0.082** |
| | Gupta et al. model | Voltage (V) | 96.1 | 89.5 | – | – | 81.6 |
| | | Issued Current (A) | 0.715 | 0.621 | – | – | 0.627 |
| | | Calculated Current (A) | 0.966 | 0.858 | – | – | 0.853 |
| | | Difference (A) | **0.251** | 0.237 | – | – | 0.226 |
| Pramac Luce MCPH P7 125W | Proposed model | Voltage (V) | 124.1 | – | 113.2 | 0.0 | – |
| | | Issued Current (A) | 0.500 | – | 0.366 | 1.589 | – |
| | | Calculated Current (A) | 0.461 | – | 0.401 | 1.554 | – |
| | | Difference (A) | **−0.039** | – | 0.035 | −0.035 | – |
| | Das model | Voltage (V) | 112.5 | – | 115.0 | 0.0 | – |
| | | Issued Current (A) | 0.965 | – | 0.258 | 1.589 | – |
| | | Calculated Current (A) | 0.913 | – | 0.288 | 1.554 | – |
| | | Difference (A) | **−0.052** | – | 0.030 | −0.035 | – |
| | Ishaque et al. model | Voltage (V) | 125.0 | – | 115.0 | 105.0 | – |
| | | Issued Current (A) | 0.450 | – | 0.258 | 0.512 | – |
| | | Calculated Current (A) | 0.307 | – | 0.173 | 0.396 | – |
| | | Difference (A) | **−0.143** | – | −0.085 | −0.116 | – |
| | Gupta et al. model | Voltage (V) | 60.0 | – | 54.8 | 46.0 | – |
| | | Issued Current (A) | 1.413 | – | 1.443 | 1.486 | – |
| | | Calculated Current (A) | 1.494 | – | 1.506 | 1.530 | – |
| | | Difference (A) | **0.081** | – | 0.063 | 0.044 | – |

Bold values indicate for each model the highest value of maximum current differences between the issued and the calculated *I–V* characteristics.

$$\Delta I = \alpha \frac{G}{G_{ref}}(T - T_{ref}) + \left(\frac{G}{G_{ref}} - 1\right) I_{sc,ref} \tag{10}$$

$$\Delta V = \beta(T - T_{ref}) - R_s \Delta I \tag{11}$$

in which $G$ and $T$ are the current values of the solar irradiance and cell temperature, respectively. The above models were used to simulate the *I–V* characteristic of thin-film Shell ST40 PV module. In Fig. 3 the *I–V* characteristics calculated with the Ishaque et al. and the Gupta et al. models are compared.

The model of Ishaque et al. was calculated assuming for the number of series cells the value of 42 [31]. Parameter $N_s$ is usually not issued by the manufactures of thin-film PV panels. Considering that $V_{oc} = 23.3$ V for the PV panel Shell ST40, a value of 0.555 V was hypothesised for the open circuit voltage of each PV cell. The procedure to evaluate parameter $R_s$ used in Eq. (11) is not described by Gupta et al. In this paper, in order to draw the *I–V* curves of Fig. 3 it was used the value of $R_s$ for which the open circuit voltage calculated at $G = 200\ W/m^2$ and $T = T_{ref}$ corresponds to the value issued by the manufacturer for the same values of solar irradiance and cell temperature. To calculate such a value of $R_s$, an iterative procedure was adopted. The procedure is based on the comparison between the value of the open voltage, issued on datasheets for $G = 200\ W/m^2$ and $T = T_{ref}$, and the value of the voltage in correspondence of which the current calculated with Eqs. (6), (10) and (11), for the same values of solar irradiance and cell temperature, results equal to zero. Starting from $R_s = 0$, the comparison is repeated incrementing $R_s$ in order to get a value of the evaluated voltage equal to the open circuit voltage extracted from the issued datasheets. Because the last term of Eq. (3) is ignored, no value of $R_p$ is required by the Gupta et al. model. The comparison between the curves of Fig. 3 shows that, even if both models are able to adequately represent the electrical behaviour of the analysed PV panel for values of the voltages smaller than the maximum power point voltage, a lack of accuracy is observed in the right part of the *I–V* characteristics.

**Table 5**
Absolute mean current and power differences between the issued and the calculated *I–V* characteristics at temperature $T = 25$ °C.

| PV panel | Absolute mean difference | | Irradiance (W/m$^2$) | | | | |
|---|---|---|---|---|---|---|---|
| | | | 200 | 400 | 600 | 800 | 1000 |
| Soltecture Linion 90 F | Current (A) | Proposed model | **0.014** | **0.014** | 0.013 | 0.007 | 0.010 |
| | | Das model | 0.019 | **0.021** | 0.019 | 0.010 | 0.010 |
| | | Ishaque et al. model | 0.063 | **0.082** | 0.078 | 0.053 | 0.064 |
| | | Gupta et al. model | 0.002 | 0.005 | 0.005 | **0.008** | **0.008** |
| | Power (W) | Proposed model | 0.680 | 0.724 | **0.827** | 0.379 | 0.667 |
| | | Das model | 0.938 | 1.109 | **1.121** | 0.583 | 0.658 |
| | | Ishaque et al. model | 3.155 | **4.593** | 4.393 | 2.818 | 3.639 |
| | | Gupta et al. model | 0.063 | 0.219 | 0.291 | **0.518** | 0.411 |
| Solar Frontier SF130-L | Current (A) | Proposed model | 0.011 | **0.015** | **0.015** | 0.009 | 0.011 |
| | | Das model | 0.010 | 0.034 | 0.060 | 0.089 | **0.111** |
| | | Ishaque et al. model | **0.064** | 0.050 | 0.038 | 0.029 | 0.023 |
| | | Gupta et al. model | 0.014 | 0.025 | 0.046 | 0.065 | **0.074** |
| | Power (W) | Proposed model | 0.710 | 1.147 | **1.181** | 0.636 | 0.782 |
| | | Das model | 0.695 | 2.678 | 4.789 | 6.885 | **8.353** |
| | | Ishaque et al. model | **3.775** | 2.817 | 2.190 | 1.613 | 1.340 |
| | | Gupta et al. model | 1.157 | 2.185 | 4.220 | 6.087 | **6.777** |
| EPV Solar EPV-42 | Current (A) | Proposed model | 0.008 | 0.007 | 0.008 | 0.010 | **0.011** |
| | | Das model | 0.010 | 0.011 | 0.013 | 0.016 | **0.022** |
| | | Ishaque et al. model | **0.055** | 0.044 | 0.039 | 0.028 | 0.039 |
| | | Gupta et al. model | 0.010 | 0.015 | 0.028 | **0.041** | 0.014 |
| | Power (W) | Proposed model | 0.363 | 0.355 | 0.357 | 0.476 | **0.483** |
| | | Das model | 0.457 | 0.518 | 0.630 | 0.775 | **1.067** |
| | | Ishaque et al. model | **2.058** | 1.787 | 1.769 | 1.344 | 1.951 |
| | | Gupta et al. model | 0.446 | 0.739 | 1.401 | **2.094** | 0.584 |
| Pramac Luce MCPH P7 125W | Current (A) | Proposed model | 0.012 | 0.013 | 0.013 | 0.015 | **0.019** |
| | | Das model | 0.009 | 0.011 | 0.013 | 0.016 | **0.024** |
| | | Ishaque et al. model | **0.152** | 0.114 | 0.073 | 0.051 | 0.052 |
| | | Gupta et al. model | 0.023 | 0.022 | 0.036 | **0.041** | 0.040 |
| | Power (W) | Proposed model | 1.059 | 1.233 | 1.224 | 1.483 | **1.942** |
| | | Das model | 0.780 | 1.028 | 1.222 | 1.632 | **2.548** |
| | | Ishaque et al. model | **12.406** | 10.123 | 6.650 | 4.938 | 5.731 |
| | | Gupta et al. model | 2.375 | 2.169 | 3.643 | **3.936** | 3.563 |
| Universe Solar Uisolar PVL-128 | Current (A) | Proposed model | 0.026 | 0.029 | **0.046** | 0.035 | 0.011 |
| | | Das model | 0.027 | 0.047 | 0.063 | 0.115 | **0.197** |
| | | Ishaque et al. model | **0.341** | 0.226 | 0.146 | 0.108 | 0.099 |
| | | Gupta et al. model | 0.060 | 0.083 | 0.171 | **0.172** | 0.111 |
| | Power (W) | Proposed model | 0.838 | 0.891 | **1.700** | 1.294 | 0.341 |
| | | Das model | 0.879 | 1.540 | 2.041 | 3.709 | **6.394** |
| | | Ishaque et al. model | **9.505** | 6.440 | 3.628 | 2.754 | 2.866 |
| | | Gupta et al. model | 2.020 | 3.198 | 7.054 | **7.135** | 4.391 |

Bold values indicate for each model the highest value of absolute mean current and power differences.

Considering that the main purpose of electrical models is to allow the most accurate representation of the *I–V* characteristics of the analysed PV panel, and because the materials of thin-film PV modules are quite different from the doped silicon wafers used to make electronic devices, the use the traditional models based on one or two diodes does not seem mandatory. Actually, different approaches may be explored in order to reach better results with a smaller mathematical complexity. Following this idea, alternative forms to describe the *I–V* characteristics of PV panels have been proposed by some authors. Akbaba et al. [32] presented a model based on the following equation:

$$I = \frac{V_{oc} - V}{A + BV^2 - CV} \tag{12}$$

where the coefficient $A$ is the ratio of the open circuit voltage $V_{oc}$ to the short-circuit current $I_{sc}$ of the cell; coefficients $B$ and $C$ are the solutions of the equation system obtained substituting in Eq. (12) the values of voltage and current of two points of the datasheet *I–V* curves whose currents are around $0.94I_{sc}$ and $0.68I_{sc}$, respectively. The model accurately represents the *I–V* curves even if, in correspondence of each value of solar irradiance and cell temperature, a new set of $A$, $B$ and $C$ has to be determined. Ortiz-Rivera et al. [33] used the following equation to describe the *I–V* characteristic of a solar panel:

$$I = \varepsilon I_{\max}\tau_i - \varepsilon I_{\max}\tau_i \exp\left(\frac{V}{b(\gamma\varepsilon + 1 - \gamma)(V_{\max} + \tau_V)} - \frac{1}{b}\right) \tag{13}$$

in which $I_{\max}$ is the ideal maximum current, defined as the current $I$ for $V = -\infty$ at SRC, and $V_{\max}$ is the value of the open circuit voltage at SRC; $\tau_i$ and $\tau_V$ are the rate of change of current and voltage with the temperature, respectively. Coefficient $\varepsilon$ is proportional to the solar irradiance, coefficient $b$ can be calculated by means of $I_{sc,ref}$ and $I_{\max}$; $\gamma$ depends on $V_{\max}$ and $V_{\min}$, which is the open-circuit voltage at 25 °C and 200 W/m$^2$. Massi Pavan et al. [34–37] introduced the following empirical expression:

$$i = i_L + z(T - 25) - \frac{e^{n[v + w(T-25)]} - 1}{e^n - 1} \tag{14}$$

where $i$ and $v$ are the normalised current and voltage defined in Eq. (1), $i_L$ is the normalised photocurrent referred to the irradiance of 1000 W/m$^2$, $w$ is the voltage-temperature coefficient divided by $V_{oc,ref}$, $z$ is the current–temperature coefficient divided by $I_{sc,ref}$ and $T$ is the solar cell temperature. The exponential factor $n$ was obtained imposing that the normalised maximum power ($v_{mp}$ $i_{mp} = V_{mp}$ $I_{mp}/V_{oc,ref}$ $I_{sc,ref}$) produced by the photovoltaic device at a

**Table 6**
Absolute mean current and power differences between the issued and the calculated *I–V* characteristics at irradiance $G = 1000\ W/m^2$.

| PV panel | Absolute mean difference | | Temperature (°C) | | | | |
|---|---|---|---|---|---|---|---|
| | | | 25 | 50 | 55 | 70 | 75 |
| Soltecture Linion 90 F | Current (A) | Proposed model | 0.010 | **0.024** | – | – | 0.010 |
| | | Das model | 0.010 | **0.022** | – | – | 0.010 |
| | | Ishaque et al. model | 0.064 | **0.077** | – | – | 0.064 |
| | | Gupta et al. model | 0.008 | **0.017** | – | – | 0.005 |
| | Power (W) | Proposed model | 0.667 | **1.330** | – | – | 0.448 |
| | | Das model | 0.658 | **1.270** | – | – | 0.448 |
| | | Ishaque et al. model | 3.639 | **3.991** | – | – | 3.052 |
| | | Gupta et al. model | 0.411 | **0.963** | – | – | 0.161 |
| Solar Frontier SF130-L | Current (A) | Proposed model | 0.011 | 0.011 | – | – | **0.020** |
| | | Das model | 0.111 | 0.140 | – | – | **0.167** |
| | | Ishaque et al. model | 0.023 | 0.038 | – | – | **0.057** |
| | | Gupta et al. model | 0.074 | 0.066 | – | – | **0.077** |
| | Power (W) | Proposed model | 0.782 | 0.600 | – | – | **0.835** |
| | | Das model | 8.353 | 9.000 | – | – | **9.405** |
| | | Ishaque et al. model | 1.340 | 2.131 | – | – | **3.143** |
| | | Gupta et al. model | **6.777** | 5.259 | – | – | 5.122 |
| Pramac Luce MCPH P7 125W | Current (A) | Proposed model | **0.019** | – | 0.013 | 0.011 | – |
| | | Das model | **0.024** | – | 0.016 | 0.021 | – |
| | | Ishaque et al. model | **0.052** | – | 0.029 | 0.034 | – |
| | | Gupta et al. model | **0.040** | – | 0.027 | 0.020 | – |
| | Power (W) | Proposed model | **1.942** | – | 1.109 | 0.568 | – |
| | | Das model | **2.548** | – | 1.345 | 1.342 | – |
| | | Ishaque et al. model | **5.731** | – | 2.741 | 3.085 | – |
| | | Gupta et al. model | **3.563** | – | 1.805 | 1.187 | – |

Bold values indicate for each model the highest value of absolute mean current and power differences.

given solar irradiance and cell temperature was equal to its fill factor at the same conditions of irradiance and cell temperature.

For simple design calculations, Karmalkar et al. [38,39] proposed the following explicit function:

$$i = 1 - (1 - \sigma)v - \sigma v^d \tag{15}$$

where $d$ and $\sigma$ were extracted using two additional points selected on the *I–V* characteristic for $v = 0.6$ and $i = 0.6$. Following the approach adopted by Akbaba et al., coefficient $d$ and $\sigma$ were calculated by solving the two independent versions of Eq. (15) written in correspondence of such additional points. The model was used to calculate the *I–V* curves and the fill factor of a number of cells at SRC. Das [40,1,41] described an explicit model, useful for design, characterisation and simple fill factor calculation, based on the following expression:

$$v^f + i^g = 1 \tag{16}$$

in which coefficients $f$ and $g$ are extracted with the relations:

$$f \approx \frac{\log(\log i_a / \log i_b)}{\log(v_a / v_b)} \quad g \approx -\frac{v_a^f}{\log(i_a)} \tag{17}$$

where $i_a$ and $i_b$ are the normalised current of two additional points on the *I–V* curve at SRC for which it is $v_a = 0.8$ and $v_b = 0.9$. Das [42] also proposed the equation:

$$i = \frac{1 - v^h}{1 + \omega v} \tag{18}$$

where coefficients $h$ and $\omega$ can be calculated by means of the values of the derivatives of the current for $v = 0$ and $v = 1$, which correspond to the short-circuit and open-circuit points of the *I–V* characteristic of the solar cell, respectively. The model parameters are valid only for the *I–V* curve for which were determined; consequently, a new set of parameters has to be calculated in correspondence of different values of solar irradiance and cell temperature.

A model, which should be valid both in the positive and negative (dark condition) voltage range, was proposed by Saetre et al. [43]. The model uses the following relations:

$$I = I_{sc}\left[1 - \left(\frac{V}{V_{oc}}\right)^{\eta}\right]^{\frac{1}{\xi}} \quad V = V_{oc}\left[1 - \left(\frac{I}{I_{sc}}\right)^{\xi}\right]^{\frac{1}{\eta}} \tag{19}$$

where parameters $\eta$ and $\xi$ can be determined by solving the two versions of the previous equations written for the values of current and voltage corresponding to the point of maximum power. Because the maximum power point varies with the solar irradiance, constant values model parameters $\eta$ and $\xi$ cannot be used.

## 3. A new equation for the *I–V* curves of thin-film PV panels

A new equation for the representation of the *I–V* characteristics of thin-film PV modules is presented in this paragraph. The relation, which is similar to the equation proposed by Das [42], is described by the following rational form:

$$i = \frac{1 - v^M}{1 + Av + v^N} \tag{20}$$

Parameters $M$, $A$ and $N$ can be calculated from the following positions:

$$\left.\frac{di}{dv}\right|_{v=0} = -A = \frac{1}{r_{sho}} \tag{21}$$

$$\left.\frac{di}{dv}\right|_{v=1} = -\frac{M}{A+2} = \frac{1}{r_{so}} \tag{22}$$

$$i_{mp,ref} = \frac{\left(1 - v_{mp,ref}^M\right)}{1 + A\,v_{mp,ref} + v_{mp,ref}^N} \tag{23}$$

in which $v_{mp,ref}$ and $i_{mp,ref}$ are the values of the normalised voltage and current in correspondence of the maximum power point at SRC, respectively; parameters $r_{hso}$ and $r_{so}$ are defined as:

$$r_{sho} = R_{sho,ref}\frac{I_{sc,ref}}{V_{oc,ref}} \tag{24}$$

$$r_{so} = R_{so,ref}\frac{I_{sc,ref}}{V_{oc,ref}} \tag{25}$$

where $R_{sho,ref}$ and $R_{so,ref}$ are the reciprocal of the slope of the $I$–$V$ characteristic in the short circuit point and the open circuit point at SRC, respectively. From Eqs. (22) and (23) it is possible to extract the expressions of coefficients $M$ and $N$:

$$M = \frac{1 - 2r_{sho}}{r_{so}r_{sho}} \tag{26}$$

$$N = \frac{\ln(1 - v_{mp,ref}^{M} + \frac{v_{mp,ref}i_{mp,ref}}{r_{sho}} - i_{mp,ref}) - \ln(i_{mp,ref})}{\ln(v_{mp,ref})} \tag{27}$$

Coefficients $A$ and $M$ are positive because $R_{sho,ref}$ and $R_{so,ref}$, and in turn $r_{sho}$ and $r_{so}$, are implicitly negative. It easy to verify that the logarithms in Eq. (27) are negative; moreover, because $v_{mp,ref}$ and $i_{mp,ref}$ are usually >0.5, the argument of the first logarithm is smaller than $i_{mp,ref}$ and coefficient $N$ is consequently positive. Actually, $N$ can be calculated only if it is:

$$1 - v_{mp,ref}^{M} + \frac{v_{mp,ref}i_{mp,ref}}{r_{sho}} - i_{mp,ref} > 0 \tag{28}$$

that, if Eq. (26) is used in Eq. (28), corresponds to the following relation:

$$r_{so} > \frac{(1 - 2r_{sho})\ln(v_{mp,ref})}{r_{sho}\ln\left[1 - i_{mp,ref}(1 - \frac{v_{mp,ref}}{r_{sho}})\right]} = r_{so,mim} \tag{29}$$

Eq. (29) is the only limitation on the use of the proposed model. As it is showed in Section 4, because real thin-film PV modules present values of the normalised series resistance much greater than $r_{so,min}$, Eq. (29) is easily satisfied. Obviously, to draw the $I$–$V$ characteristics of a PV panel it is necessary to pass from normalised current $i$ and voltage $v$ to real current $I$ and voltage $V$ at SRC:

$$I = I_{sc,ref}\frac{1 - \left(\frac{V}{V_{oc,ref}}\right)^{M}}{1 + A\frac{V}{V_{oc,ref}} + \left(\frac{V}{V_{oc,ref}}\right)^{N}} \tag{30}$$

Moreover, because the model has to be able to represent the $I$–$V$ characteristics also for conditions different from SRC, it is necessary to generalize Eq. (30) considering the variations of the model parameters with solar irradiance $G$ and cell temperature $T$. Such a purpose can be adequately achieved using the following equation:

$$I = \alpha_G\left[I_{sc,ref} + \alpha(T - T_{ref})\right]\frac{1 - \left[\frac{V - \beta(T - T_{ref})}{V_{oc}(G)}\right]^{M(G)}}{1 + A(G)\frac{V - \beta(T - T_{ref})}{V_{oc}(G)} + \left[\frac{V - \beta(T - T_{ref})}{V_{oc}(G)}\right]^{N}} \tag{31}$$

where quantity $\alpha_G = G/G_{ref}$ denotes the ratio between the generic solar irradiance and the solar irradiance at SRC. Because the slopes of the $I$–$V$ characteristics in the short circuit point and the open circuit point significantly change with the solar irradiance, coefficients $A(G)$ and $M(G)$ have to be calculated by means of Eqs. (21) and (26) using the following equations in place of Eqs. (24) and (25):

$$r_{sho} = R_{sho}(G)\frac{\alpha_G I_{sc,ref}}{V_{oc}(G)} \tag{32}$$

$$r_{so} = R_{so}(G)\frac{\alpha_G I_{sc,ref}}{V_{oc}(G)} \tag{33}$$

in which $V_{oc}(G)$, $R_{sho}(G)$ and $R_{so}(G)$ describe the variation of the open circuit voltage and of the slopes of the $I$–$V$ characteristics at the extremes of the curves. Coefficient $N$ can be kept constant.

If very accurate results are required, the variations of $V_{oc}$, $R_{sho}$ and $R_{so}$ extracted from the $I$–$V$ characteristics issued by the manufacturer should be used because they are peculiar to the analysed PV panel. Nevertheless, a good accuracy can be also reached by means of some empirical relations that were found on the basis of the $I$–$V$ characteristics issued on the Internet by 25 manufacturers for 60 models of thin-film PV panels. Using the data listed in Table A1 of the Appendix, the following relation, which permits to interpolate the values of the open circuit voltage between 200 and 1000 w/m$^2$, was defined:

$$V_{oc}(G) = V_{ocref}\{C_1[\ln(\alpha_G)]^3 + C_2[\ln(\alpha_G)]^2 + C_3 ln(\alpha_G) + 1\} \tag{34}$$

where:

$$C_1 = -0.022479\frac{V_{oc,200}}{V_{oc,ref}} + 0.020312 \tag{35}$$

$$C_2 = -0.357722\frac{V_{oc,200}}{V_{oc,ref}} + 0.320504 \tag{36}$$

$$C_3 = -1.138838\frac{V_{oc,200}}{V_{oc,ref}} + 1.084553 \tag{37}$$

in which $V_{oc,200}$ is the value of the open circuit voltage referred to the $I$–$V$ curve at $G = 200$ W/m$^2$ and $T = T_{ref}$, which can be extracted from the $I$–$V$ characteristics issued by manufacturers. Fig. 4 illustrates the correspondence between the issued values of $V_{oc}$ and the values calculated with Eq. (34).

Because a point on the identity line corresponds to a perfect correspondence between issued and calculated values, the markers lying under the identity line indicate calculated values that are smaller than the values extracted from the issued characteristics; the opposite is for the values represented by the markers that are above the identity line. The distribution of the percentage error due to the use of Eq. (34) is depicted in Fig. 5.

An error less than 1% affects the open circuit voltage calculated for 77.6% 73.5% and 94.0%, of the surveyed $I$–$V$ curves at 400, 600 and 800 W/m$^2$, respectively; the root mean square relative errors are 1.05%, 0.93% and 0.52% at 400, 600 and 800 W/m$^2$, respectively.

In order to define $R_{sho}(G)$ and $R_{so}(G)$, the reciprocal of slopes of the $I$–$V$ curve in correspondence of the short circuit and open circuit points were extracted from the issued $I$–$V$ characteristics using the graphical procedure described in [44]. It was found that $R_{sho}$ of thin-film PV panels follows the following relation, which is similar to that one proposed by some authors [45–47] for the shunt resistance of the one-diode equivalent model:

$$R_{sho}(G) = \frac{R_{sho,ref}}{\alpha_G} \tag{38}$$

For $R_{so}(G)$, whose normalised values extracted from the measured characteristics are listed in Table A2 of Appendix, a different approach was necessary. Accurate calculations of $R_{so}(G)$ can be obtained by means of the following equation:

$$R_{so}(G) = R_{so,ref}\left(\frac{D_1}{\alpha_G} + D_2\right) \tag{39}$$

where the values of coefficients $C_1$ and $C_2$, which depend on the thin-film technology, are:

- Amorphous: $D_1 = 0.800951$ $D_2 = 0.199049$
- Tandem: $D_1 = 0.639077$ $D_2 = 0.360923$
- Triple: $D_1 = 0.433214$ $D_2 = 0.566786$
- CIS: $D_1 = 0.407039$ $D_2 = 0.592961$
- CIGS: $D_1 = 0.651625$ $D_2 = 0.348375$

Fig. 6 illustrates the correspondence between the values of $R_{so}$ extracted from the $I$–$V$ characteristics at various levels of solar irradiance and the values calculated with Eq. (39).

In Fig. 7 the distribution of the percentage error due to the use of Eq. (39) is depicted.

An error less than 20% affects the values of $R_{so}$ calculated for 87.0%, 82.1%, 83.9% and 96.5% of the surveyed $I$–$V$ characteristics at 200, 400, 600 and 800 W/m$^2$, respectively. The root mean square relative errors in evaluating $R_{so}$ are 13.65%, 17.51%, 15.08% and 9.67% at 200, 400, 600 and 800 W/m$^2$, respectively.

## 4. Application of the model and analysis of the results

With the aim of verifying the effectiveness of the proposed model, a comparison with the Ishaque et al. and the Gupta et al. models was made using the $I$–$V$ characteristics of various types of thin-film PV panels. The study does not include the CdTe technology because it was impossible to find any $I$–$V$ characteristic, even though the datasheets issued on the Internet by more than 200 manufacturers of thin-film PV panels were carefully examined. For amorphous and triple junction PV panels, only the $I$–$V$ curves at $T = 25$ °C were found. The performance data of the analysed thin-film PV modules are listed in Table 1.

For the sake of precision, the data listed in Table 1 were accurately extracted from the graphs provided by manufacturers. For this reason, some small differences with the data listed in the Appendix may be observed. Table 2, which lists the values of the parameters evaluated with the proposed model, permits to verify that Eq. (29) is always satisfied by the analysed PV panels.

Fig. 8 shows the comparison between the values of $V_{oc}(G)$ extracted from the issued characteristics of the analysed PV panels and the values calculated with Eq. (34).

Fig. 9 shows the comparison between the values of parameter $R_{so}$ extracted from the measured characteristics and the values calculated with Eq. (39).

In Figs. 10–13, the $I$–$V$ curves evaluated with the proposed model and the characteristics calculated with the Das, the Gupta et al. and the Ishaque et al. models are compared with the data issued on the manufacturer's datasheets. To calculate the $I$–$V$ characteristics with the Das model for conditions different from the SRC, the same procedure to extend the proposed model to any condition was used. It can be observed that for each value of the solar irradiance, or temperature, the curves calculated with the proposed model are very similar to the issued characteristics.

The Das model yields a good representation of the STC performance curves of the Soltecture panels; the lack of the third parameter, which is used by the proposed model in order to contain the maximum power point, does not permit to reach adequate results for the other PV modules. The Gupta et al. model is accurate with the Soltecture panel, whereas it overestimates the current of the Solar Frontier, EPV and Universe Solar panels for values of the voltage greater than the maximum power point voltage. For the Pramac panel, and partially for the EPV panel, an overestimate of the current calculated for values of the voltage smaller than the maximum power point voltage is also observed. More evident inaccuracies are present in the $I$–$V$ curves calculated with the Ishaque et al. model. Actually, because the model only considers the perfect correspondence with the maximum power point at SRC, no attempt was made to control the shape of the calculated curves far from this point. The Ishaque et al. model generally underestimates the current at SRC of all the analysed PV panels for values of the voltage far from the maximum power point voltage. At the lowest values of the solar irradiance, the greatest inaccuracies are present. An evident lack of correspondence between the calculated and issued values of the open circuit voltage is also observed. The inaccuracy of the open voltages value may be due to the number of series cells $N_s$ used to calculate $V_T$ in Eqs. (4) and (5), which was set considering the value of the open circuit voltage of 0.555 V/cell used by Ishaque et al. for the panel Shell ST40. Tables 3 and 4 list the maximum differences of current between the measured and the calculated data.

At a constant temperature of $T = 25$ °C, the maximum differences for current are achieved with the Universe Solar panel. The maximum differences are −0.482 A for the Das model, −0.483 A for the Ishaque et al. model, 0.545 A for the Gupta et al. model and 0.102 A for the proposed model. If compared to the issued values of current at the maximum power point at SRC, these differences correspond to a percentage error of −12.36%, −12.38%, 13.97%, and 2.62%, respectively.

At a constant irradiance of $G = 1000$ W/m$^2$, the maximum differences for current are achieved for the Soltecture panel when the Ishaque et al. and the proposed model are used; with the Das and the Gupta et al. model, the maximum difference for current is observed for the Solar Frontier panel. The maximum differences are −0.331 A for the Das model, −0.248 A for the Ishaque et al. model, 0.251 A for the Gupta et al. model and −0.097 A for the proposed model. If compared to the issued values of current at the maximum power point at SRC, these differences correspond to a percentage error of −18.39%, −15.60%, 13.94%, and −6.10%, respectively. Tables 5 and 6 list the absolute mean differences of current and of power between the measured and the calculated data.

At a constant temperature of $T = 25$ °C, the maximum absolute mean differences for current are achieved with the Universe Solar panel. The maximum absolute mean differences for current are 0.197 A for the Das model, 0.341 A for the Ishaque et al. model, 0.172 A for the Gupta et al. model and 0.046 A for the proposed model. If compared to the issued values of current at the maximum power point at SRC, these differences correspond to a percentage error of 5.05%, 8.74%, 4.41%, and 1.18%, respectively. The maximum absolute mean differences for power are achieved for the Pramac panel when the Ishaque et al. and the proposed model are used; with the Gupta et al. model, the maximum absolute mean differences for power is observed for the Universe Solar panel. The Das model reaches the maximum absolute mean differences with tha Solar Frontier panel. The absolute mean differences for power are 8.353 W for the Das model, 12.406 W A for the Ishaque et al. model, 7.135 W for the Gupta et al. model and 1.942 W for the proposed model. If compared to the issued values of the maximum power at SRC, these differences correspond to a percentage error of 6.19%, 10.25%, 5.63%, and 1.60%, respectively.

At a constant irradiance of $G = 1000$ W/m$^2$, The maximum absolute mean differences for current are achieved for the Soltecture panel when the Ishaque et al. and the proposed model are used; with the Das and the Gupta et al. model, the maximum absolute mean differences for current is observed for the Solar Frontier panel. The maximum absolute mean differences for current are 0.167 A for the Das model, 0.077 A for the Ishaque et al. model, 0.077 A for the Gupta et al. model and 0.024 A for the proposed model. If compared to the issued values of current at the maximum power point at SRC, these differences correspond to a percentage error of 9.28%, 4.84%, 4.28%, and 1.51%, respectively. The maximum absolute mean differences for power are achieved for the Pramac panel when the Ishaque et al. and the proposed model are used; with the Das and the Gupta et al. model, the maximum absolute mean differences for power is observed for the Solar Frontier panel. The absolute mean differences for power are 9.405 W for the Das model, 5.731 W for the Ishaque et al. model, 6.777 W for the Gupta et al. model and 1.942 W for the proposed model. If compared to the issued values of the maximum power at SRC, these differences correspond to a percentage error of 6.97%, 4.74%, 5.02%, and 1.60%, respectively.

The accuracy of the proposed model, which is always more precise than the Ishaque et al. and the Gupta et al. models is quite satisfactory. Even in worst case, the proposed model calculates the $I$–$V$

**Table A1**
Values of the open circuit voltage at various solar irradiances.

| Manufacturer | Model | Type | Open circuit voltage $V_{oc}$ (V) Solar irradiance $G$ (kW/m$^2$) | | | | | Scaled open circuit voltage $V_{oc}/V_{oc.ref}$ Solar irradiance $G$ (kW/m$^2$) | | | | |
|---|---|---|---|---|---|---|---|---|---|---|---|---|
| | | | 1.00 | 0.80 | 0.60 | 0.40 | 0.20 | 1.00 | 0.80 | 0.60 | 0.40 | 0.20 |
| Astom | ASSG100 | Amorph. | 92.0 | 90.4 | 88.6 | 86.2 | 82.7 | 1.000 | 0.982 | 0.963 | 0.937 | 0.899 |
| Astronergy | CHSM 5011T 130 | Tandem | 170.0 | 169.2 | 167.9 | 159.7 | 152.3 | 1.000 | 0.995 | 0.988 | 0.940 | 0.896 |
| Bangkok Solar | BS-52 | Amorph. | 93.6 | 92.6 | 91.2 | 89.2 | 85.0 | 1.000 | 0.990 | 0.975 | 0.953 | 0.908 |
| Baoding Tianwei | TW-SE95 | Amorph. | 137.0 | 133.4 | 130.8 | 126.9 | 125.2 | 1.000 | 0.974 | 0.955 | 0.927 | 0.914 |
| Baoding Tianwei | TW-SF-W105 | Amorph. | 137.0 | 134.9 | 132.2 | 128.1 | 126.6 | 1.000 | 0.985 | 0.965 | 0.935 | 0.924 |
| DuPont Apollo | DA100 | Amorph. | 97.0 | 95.9 | 94.5 | 92.6 | 88.9 | 1.000 | 0.989 | 0.974 | 0.954 | 0.917 |
| DuPont Apollo | DA130 | Tandem | 154.0 | 151.9 | 149.0 | 145.1 | 138.9 | 1.000 | 0.986 | 0.967 | 0.942 | 0.902 |
| Easy BIPV | NT-150AG | Tandem | 85.5 | 82.4 | 80.3 | 78.0 | 72.2 | 1.000 | 0.964 | 0.939 | 0.912 | 0.844 |
| ENN | EST-480 | Tandem | 286.0 | 281.0 | 274.8 | 266.5 | 254.0 | 1.000 | 0.982 | 0.961 | 0.932 | 0.888 |
| Epvsolar | EPV-40 | Amorph. | 59.0 | 58.7 | 58.5 | 56.1 | 53.7 | 1.000 | 0.995 | 0.991 | 0.951 | 0.910 |
| Epvsolar | EPV-42 | Amorph. | 60.0 | 59.8 | 59.5 | 57.2 | 53.1 | 1.000 | 0.996 | 0.991 | 0.953 | 0.885 |
| Epvsolar | EPV-50 | Amorph. | 60.0 | 59.7 | 59.4 | 58.6 | 57.2 | 1.000 | 0.995 | 0.990 | 0.977 | 0.953 |
| Kaneka | U-EA110 | Tandem | 71.0 | 70.1 | 68.9 | 67.2 | 64.0 | 1.000 | 0.988 | 0.970 | 0.947 | 0.901 |
| Mitsubishi | MT110 | Tandem | 131.0 | 129.4 | 126.7 | 123.7 | – | 1.000 | 0.988 | 0.968 | 0.944 | – |
| Mitsubishi | MT120 | Tandem | 131.0 | 129.4 | 127.0 | 124.1 | – | 1.000 | 0.988 | 0.969 | 0.947 | – |
| Mitsubishi | MT130 | Tandem | 130.0 | 128.6 | 125.8 | 123.0 | – | 1.000 | 0.989 | 0.968 | 0.946 | – |
| NexPower | NT-150AX | Tandem | 85.5 | 83.9 | 82.2 | 80.3 | 76.4 | 1.000 | 0.982 | 0.961 | 0.939 | 0.893 |
| Pramac Luce | MCPH P7 125W | Tandem | 131.4 | 129.4 | 127.3 | 123.9 | 118.6 | 1.000 | 0.985 | 0.969 | 0.943 | 0.903 |
| Q.Cells | SL1-80 | CIGS | 72.8 | – | – | – | 66.3 | 1.000 | – | – | – | 0.910 |
| Q.Cells | UF 95 | CIGS | 78.0 | – | – | – | 71.8 | 1.000 | – | – | – | 0.921 |
| Q.Cells | UF L 115 | CIGS | 95.1 | – | – | – | 87.4 | 1.000 | – | – | – | 0.919 |
| Setsolar | TF90 | Amorph. | 98.0 | 96.2 | – | – | 88.2 | 1.000 | 0.982 | – | – | 0.900 |
| Sharp | NA-F121 (G5) | Tandem | 59.2 | 58.9 | 57.8 | 56.3 | 52.5 | 1.000 | 0.995 | 0.976 | 0.951 | 0.887 |
| Sharp | NA-E125G5 | Tandem | 59.7 | 59.2 | 58.1 | 56.7 | 54.4 | 1.000 | 0.991 | 0.973 | 0.949 | 0.911 |
| Sharp | NA-F135 (G5) | Tandem | 61.3 | 60.7 | 59.6 | 58.4 | 57.0 | 1.000 | 0.990 | 0.972 | 0.953 | 0.929 |
| Shell | ST5 | CIS | 22.9 | 22.4 | 21.7 | 20.7 | 19.1 | 1.000 | 0.976 | 0.947 | 0.904 | 0.834 |
| Shell | ST10 | CIS | 22.9 | 22.6 | 22.1 | 21.7 | 20.9 | 1.000 | 0.987 | 0.967 | 0.949 | 0.912 |
| Shell | ST20 | CIS | 22.9 | 22.5 | 22.0 | 21.3 | 21.0 | 1.000 | 0.983 | 0.962 | 0.929 | 0.918 |
| Shell | ST36 | CIS | 22.9 | 22.3 | 21.7 | 20.7 | 19.1 | 1.000 | 0.973 | 0.948 | 0.904 | 0.832 |
| Shell | ST40 | CIS | 23.3 | 22.8 | 22.3 | 21.6 | 20.2 | 1.000 | 0.978 | 0.957 | 0.925 | 0.867 |
| Solar Frontier | SF80-EX-B | CIS | 56.5 | 56.0 | 55.3 | 53.7 | – | 1.000 | 0.991 | 0.979 | 0.950 | – |
| Solar Frontier | SF130-L | CIS | 106.0 | 104.8 | 103.2 | 100.8 | 95.6 | 1.000 | 0.988 | 0.973 | 0.951 | 0.902 |
| Solar Frontier | SF140-L | CIS | 109.0 | 107.6 | 106.1 | 103.7 | 98.5 | 1.000 | 0.987 | 0.973 | 0.951 | 0.903 |
| Solar Frontier | SF145-L | CIS | 110.0 | 108.8 | 107.0 | 104.7 | 99.5 | 1.000 | 0.989 | 0.973 | 0.952 | 0.904 |
| Solar Frontier | SF150-L | CIS | 110.0 | 108.8 | 106.7 | 104.3 | 99.9 | 1.000 | 0.989 | 0.970 | 0.948 | 0.909 |
| Solar Frontier | SF160-S | CIS | 110.0 | 109.0 | 106.9 | 104.0 | 100.1 | 1.000 | 0.991 | 0.972 | 0.946 | 0.910 |
| Solar Frontier | SF165-S | CIS | 110.0 | 109.0 | 106.9 | 104.0 | 99.8 | 1.000 | 0.991 | 0.972 | 0.946 | 0.908 |
| Solar Frontier | SF170-S | CIS | 112.0 | 111.0 | 108.9 | 105.9 | 101.9 | 1.000 | 0.991 | 0.973 | 0.945 | 0.910 |
| Solopower | SF1 85 | CIGS | 45.4 | 44.4 | 43.1 | 41.1 | 37.6 | 1.000 | 0.978 | 0.949 | 0.906 | 0.828 |
| Soltecture | Linion 90 | CIGS | 72.2 | 70.4 | 68.8 | 66.0 | 61.0 | 1.000 | 0.976 | 0.953 | 0.914 | 0.844 |
| Sulfurcell | SCG60-HV-F | CIS | 52.1 | 51.5 | 50.3 | 48.6 | 46.6 | 1.000 | 0.988 | 0.965 | 0.932 | 0.895 |
| Sun Solar USA | Tandem 110 | Tandem | 128.0 | 126.3 | 123.8 | – | – | 1.000 | 0.987 | 0.967 | – | – |
| Sun Well | WD-125 | Amorph. | 91.0 | 90.0 | 89.0 | 87.0 | 84.0 | 1.000 | 0.989 | 0.978 | 0.956 | 0.923 |
| Sungen | SG-BIPV-GG-75 | Amorph. | 90.0 | 89.4 | 89.0 | 87.9 | 84.9 | 1.000 | 0.993 | 0.988 | 0.977 | 0.943 |
| Sungen | SG-NH95-GG | Amorph. | 92.4 | 90.5 | 88.7 | 86.7 | 83.0 | 1.000 | 0.980 | 0.960 | 0.938 | 0.899 |
| Sungen | SG-NH95-GS | Amorph. | 95.8 | 93.8 | 91.8 | 89.8 | 86.2 | 1.000 | 0.979 | 0.958 | 0.937 | 0.900 |
| Sungen | SG-HN100-GG | Amorph. | 92.0 | 91.7 | 91.3 | 90.3 | 86.8 | 1.000 | 0.997 | 0.992 | 0.982 | 0.943 |
| Sungen | SG-HN100-GGLV | Amorph. | 38.6 | 38.4 | 38.3 | 37.8 | 36.6 | 1.000 | 0.996 | 0.992 | 0.980 | 0.948 |
| Suntech | STP090Ts-AA | Amorph. | 93.8 | 92.9 | 92.0 | 90.5 | 86.7 | 1.000 | 0.991 | 0.981 | 0.965 | 0.924 |
| Suntech | STP0180Ts-BA | Amorph. | 187.6 | 185.9 | 183.9 | 181.0 | 173.5 | 1.000 | 0.991 | 0.981 | 0.965 | 0.925 |
| Suntech | STP0180Ts-CA | Amorph. | 95.7 | 94.9 | 93.8 | 92.4 | 88.4 | 1.000 | 0.992 | 0.981 | 0.966 | 0.924 |
| Suntech | STP0360Ts-DA | Amorph. | 187.6 | 185.9 | 184.4 | 181.4 | 173.4 | 1.000 | 0.991 | 0.983 | 0.967 | 0.925 |
| Tsmc Solar | TS-145C1 | CIGS | 61.5 | 61.1 | 60.4 | 59.1 | 56.0 | 1.000 | 0.993 | 0.982 | 0.962 | 0.911 |
| Universe Solar | Uisolar PVL-31 | Triple j. | 10.5 | 10.4 | 10.2 | 10.1 | – | 1.000 | 0.990 | 0.975 | 0.957 | – |
| Universe Solar | Uisolar PVL-33 | Triple j. | 10.5 | 10.4 | 10.2 | 10.0 | – | 1.000 | 0.990 | 0.974 | 0.957 | – |
| Universe Solar | Uisolar PVL-68 | Triple j. | 23.1 | 22.8 | 22.6 | 22.1 | 21.2 | 1.000 | 0.989 | 0.977 | 0.955 | 0.917 |
| Universe Solar | Uisolar PVL-72 | Triple j. | 23.1 | 22.8 | 22.5 | 22.1 | 21.2 | 1.000 | 0.989 | 0.976 | 0.956 | 0.916 |
| Universe Solar | Uisolar PVL-128 | Triple j. | 47.6 | 47.1 | 46.5 | 45.6 | 44.0 | 1.000 | 0.990 | 0.977 | 0.958 | 0.925 |
| Universe Solar | Uisolar PVL-136 | Triple j. | 46.2 | 45.7 | 45.0 | 43.9 | 42.0 | 1.000 | 0.988 | 0.974 | 0.950 | 0.909 |
| Universe Solar | UisolarPVL-144 | Triple j. | 46.2 | 45.6 | 45.0 | 44.2 | 42.3 | 1.000 | 0.988 | 0.974 | 0.956 | 0.916 |

characteristics with an error smaller than the data tolerance usually declared by the manufacturer, which usually is +10/−5% for maximum power at SRC.

## 5. Conclusions

A new model suited to thin-film PV modules is described. The model is based on a rational function that does not contain any implicit exponential form and that allows an easy computation of the model parameters. Two of the three parameters of the model are evaluated imposing on both the calculated *I–V* characteristics and those issued by manufacturers the condition of equality of the curve derivative in the short circuit and open circuit points at SRC. The third parameter is obtained assuming that the calculated *I–V* characteristic contains the maximum power point of the simulated PV panel at SRC.

The capability of the proposed model to calculate the *I–V* characteristics was tested by comparing the results with the data

**Table A2**
Values of parameter $R_{so}$ at various solar irradiances.

| Manufacturer | Model | Type | $V_{oc,ref}$ (V) | $I_{sc,ref}$ (A) | $V_{oc,ref}/I_{sc,ref}$ (Ω) | Parameter $R_{so}$ (Ω) Solar irradiance $G$ (kW/m$^2$) | | | | |
|---|---|---|---|---|---|---|---|---|---|---|
| | | | | | | 1.00 | 0.80 | 0.60 | 0.40 | 0.20 |
| Astom | ASSG100 | Amorph. | 92.00 | 1.74 | 52.874 | −8.788 | −11.446 | −12.454 | −22.343 | −37.379 |
| Astronergy | CHSM 5011T 130 | Tandem | 170.00 | 1.14 | 149.123 | −21.983 | −25.786 | −34.412 | −48.650 | −68.587 |
| Bangkok Solar | BS-52 | Amorph. | 93.60 | 0.88 | 106.364 | −14.026 | −17.236 | −21.000 | −33.962 | −68.102 |
| Baoding Tianwei | TW-SE95 | Amorph. | 137.00 | 1.16 | 118.103 | −12.976 | −16.565 | −22.385 | −32.923 | −52.180 |
| Baoding Tianwei | TW-SF-W105 | Amorph. | 137.00 | 1.19 | 115.126 | −13.320 | −17.083 | −21.934 | −32.901 | −56.502 |
| DuPont Apollo | DA100 | Amorph. | 97.00 | 1.77 | 54.802 | −8.179 | −10.493 | −14.038 | −18.332 | −37.453 |
| DuPont Apollo | DA130 | Tandem | 154.00 | 1.40 | 110.000 | −15.103 | −22.964 | −30.729 | −44.932 | −60.160 |
| Easy BIPV | NT-150AG | Tandem | 85.50 | 2.54 | 33.661 | −7.428 | −8.657 | −10.247 | −15.044 | −28.008 |
| ENN | EST-480 | Tandem | 286.00 | 2.66 | 107.519 | −25.256 | −27.808 | −38.261 | −55.226 | 105.446 |
| Epvsolar | EPV-40 | Amorph. | 59.00 | 1.17 | 50.427 | −10.318 | −14.409 | −17.175 | −25.364 | −34.242 |
| Epvsolar | EPV-42 | Amorph. | 60.00 | 1.18 | 50.847 | −10.399 | −14.267 | −15.853 | −23.779 | −44.387 |
| Epvsolar | EPV-50 | Amorph. | 60.00 | 1.41 | 42.553 | −9.181 | −11.800 | −13.561 | −17.904 | −31.353 |
| Kaneka | U-EA110 | Tandem | 71.00 | 2.50 | 28.400 | −5.252 | −6.046 | −6.497 | −9.156 | −13.820 |
| Mitsubishi | MT110 | Tandem | 131.00 | 1.30 | 100.769 | −16.558 | −19.711 | −26.325 | −42.270 | – |
| Mitsubishi | MT120 | Tandem | 131.00 | 1.42 | 92.254 | −14.544 | −17.775 | −24.842 | −35.509 | – |
| Mitsubishi | MT130 | Tandem | 130.00 | 1.59 | 81.761 | −13.426 | −16.978 | −22.358 | −35.196 | – |
| NexPower | NT-150AX | Tandem | 85.50 | 2.54 | 33.661 | −6.257 | −8.024 | −9.628 | −12.172 | −23.837 |
| Pramac Luce | MCPH P7 125 W | Tandem | 131.40 | 1.54 | 85.325 | −14.290 | −16.534 | −19.569 | −24.554 | −45.135 |
| Q.Cells | SL1–80 | CIGS | 72.80 | 1.60 | 45.500 | −5.434 | – | – | – | −20.112 |
| Q.Cells | UF 95 | CIGS | 78.00 | 1.68 | 46.429 | −6.113 | – | – | – | −21.723 |
| Q.Cells | UF L 115 | CIGS | 95.10 | 1.69 | 56.272 | −6.080 | – | – | – | −21.774 |
| Setsolar | TF90 | Amorph. | 98.00 | 1.59 | 61.635 | −9.387 | −10.640 | – | – | −35.403 |
| Sharp | NA-F121 (G5) | Tandem | 59.20 | 3.35 | 17.672 | −2.974 | −3.588 | −3.386 | −6.027 | −7.876 |
| Sharp | NA-E125G5 | Tandem | 59.70 | 3.37 | 17.715 | −2.532 | −2.968 | −4.737 | −4.736 | −9.121 |
| Sharp | NA-F135 (G5) | Tandem | 61.30 | 3.41 | 17.977 | −2.727 | −2.982 | −3.297 | −4.857 | −9.184 |
| Shell | ST5 | CIS | 22.90 | 0.39 | 58.718 | −16.997 | −18.543 | −21.763 | −24.297 | −39.560 |
| Shell | ST10 | CIS | 22.90 | 0.77 | 29.740 | −5.145 | −5.443 | −6.239 | −8.779 | −12.291 |
| Shell | ST20 | CIS | 22.90 | 1.54 | 14.870 | −3.700 | −4.496 | −5.303 | −6.678 | −8.988 |
| Shell | ST36 | CIS | 22.90 | 2.68 | 8.545 | −2.273 | −2.639 | −3.324 | −3.502 | −5.704 |
| Shell | ST40 | CIS | 23.30 | 2.68 | 8.694 | −1.890 | −1.913 | −2.278 | −2.830 | −4.467 |
| Solar Frontier | SF80-EX-B | CIS | 56.50 | 2.26 | 25.000 | −6.561 | −7.343 | −8.099 | −9.077 | – |
| Solar Frontier | SF130-L | CIS | 106.00 | 2.10 | 50.476 | −14.541 | −15.216 | −16.182 | −21.678 | −41.330 |
| Solar Frontier | SF140-L | CIS | 109.00 | 2.10 | 51.905 | −14.378 | −15.636 | −17.124 | −23.364 | −43.853 |
| Solar Frontier | SF145-L | CIS | 110.00 | 2.10 | 52.381 | −14.517 | −15.683 | −18.482 | −23.760 | −39.977 |
| Solar Frontier | SF150-L | CIS | 110.00 | 2.10 | 52.381 | −13.178 | −14.584 | −15.399 | −26.702 | −37.344 |
| Solar Frontier | SF160-S | CIS | 110.00 | 2.20 | 50.000 | −9.556 | −10.971 | −12.639 | −17.410 | −23.988 |
| Solar Frontier | SF165-S | CIS | 110.00 | 2.20 | 50.000 | −8.652 | −10.446 | −11.669 | −14.740 | −20.410 |
| Solar Frontier | SF170-S | CIS | 112.00 | 2.20 | 50.909 | −9.040 | −9.497 | −10.562 | −13.813 | −20.164 |
| Solopower | SF1 85 | CIGS | 45.40 | 3.10 | 14.645 | −2.952 | −3.605 | −3.933 | −6.740 | −11.379 |
| Soltecture | Linion 90 | CIGS | 72.20 | 1.80 | 40.111 | −4.547 | −5.449 | −6.914 | −10.585 | −17.838 |
| Sulfurcell | SCG60-HV-F | CIS | 52.10 | 1.74 | 29.943 | −4.235 | −4.659 | −6.748 | −7.599 | −14.245 |
| Sun Solar USA | Tandem 110 | Tandem | 128.00 | 1.37 | 93.431 | −10.543 | −14.140 | −17.638 | – | – |
| Sun Well | WD-125 | Amorph. | 91.00 | 2.22 | 40.991 | −7.352 | −7.941 | −9.261 | −12.678 | −23.057 |
| Sungen | SG-BIPV-GG-75 | Amorph. | 90.00 | 1.50 | 60.000 | −7.990 | −9.273 | −12.335 | −17.054 | −36.149 |
| Sungen | SG-NH95-GG | Amorph. | 92.40 | 1.69 | 54.675 | −7.388 | −10.111 | −12.244 | −20.265 | −28.076 |
| Sungen | SG-NH95-GS | Amorph. | 95.80 | 1.71 | 56.023 | −8.042 | −9.589 | −10.356 | −18.480 | −29.272 |
| Sungen | SG-HN100-GG | Amorph. | 92.00 | 1.74 | 52.874 | −5.044 | −6.246 | −10.626 | −13.643 | −20.464 |
| Sungen | SG-HN100-GGLV | Amorph. | 38.60 | 4.13 | 9.346 | −1.279 | −1.350 | −2.007 | −2.388 | −4.360 |
| Suntech | STP090Ts-AA | Amorph. | 93.80 | 1.50 | 62.533 | −4.488 | −5.491 | −6.112 | −16.381 | −20.912 |
| Suntech | STP0180Ts-BA | Amorph. | 187.60 | 1.50 | 125.067 | −10.405 | −22.551 | −24.294 | −39.788 | −41.558 |
| Suntech | STP0180Ts-CA | Amorph. | 93.80 | 3.00 | 31.267 | −2.235 | −2.279 | −2.538 | −8.070 | −9.375 |
| Suntech | STP0360Ts-DA | Amorph. | 187.60 | 3.00 | 62.533 | −4.471 | −6.017 | −12.088 | −16.140 | −20.138 |
| Tsmc Solar | TS-145C1 | CIGS | 61.50 | 3.44 | 17.878 | −3.454 | −3.986 | −4.244 | −5.019 | −10.383 |
| Universe Solar | Uisolar PVL-31 | Triple j. | 10.50 | 5.10 | 2.059 | −0.620 | −0.709 | −0.896 | −1.245 | – |
| Universe Solar | Uisolar PVL-33 | Triple j. | 10.50 | 5.30 | 1.981 | −0.505 | −0.583 | −0.740 | −0.968 | – |
| Universe Solar | Uisolar PVL-68 | Triple j. | 23.10 | 5.10 | 4.529 | −1.435 | −1.788 | −2.120 | −2.744 | −3.713 |
| Universe Solar | Uisolar PVL-72 | Triple j. | 23.10 | 5.30 | 4.358 | −1.140 | −1.394 | −1.741 | −2.165 | −2.760 |
| Universe Solar | Uisolar PVL-128 | Triple j. | 47.60 | 4.80 | 9.917 | −3.013 | −3.551 | −4.206 | −4.408 | −7.620 |
| Universe Solar | Uisolar PVL-136 | Triple j. | 46.20 | 5.10 | 9.059 | −2.417 | −2.983 | −3.596 | −4.036 | −5.818 |
| Universe Solar | UisolarPVL-144 | Triple j. | 46.20 | 5.30 | 8.717 | −2.118 | −2.434 | −2.992 | −3.851 | −5.587 |

issued by four different manufacturers of thin-film PV panels. Furthermore a comparison with the model proposed by Das, which is based on an equivalent rational function, and the two-diode models used by Ishaque et al. and the Gupta et al. to simulate the *I–V* characteristics of a CIS PV panel was made. The proposed model always resulted more precise than the Das, the Ishaque et al. and the Gupta et al. models. At a constant temperature of $T = 25$ °C, the maximum absolute mean differences between current and power values calculated by the proposed model and the issued values are 1.18% and 1.60% of the nominal current and power at the maximum power point, respectively. At a constant irradiance of $G = 1000$ W/m$^2$, the maximum absolute mean differences are 1.51% and 1.60% of the nominal current and power at the maximum power point, respectively. The results of calculations give account of the reliability of the proposed model. The differences between the calculated and the issued data are always less than the data tolerance usually declared by the manufacturers.

## Appendix A

See Tables A1 and A2.

## References


[1] Zhu H, Kalkan AK, Hou J, Fonash SJ. Applications of AMPS-1D for solar cell simulation. AIP Conf Proc 1999;462:309–14.
[2] Block M, Bonnet D, Zetzsche F. Modeling of multilayer amorphous thin film silicon germanium single and tandem solar cells. In: Conference record of the twenty second IEEE Photovoltaic Specialists Conference, vol. 2, 1991. p. 1275–80.
[3] Lee JY, Gray JL. Numerical modeling of CdS/CdTe solar cells: a parameter study. In: Conference record of the twenty second IEEE Photovoltaic Specialists Conference, vol. 2. 1991. p. 1151–5.
[4] Lee JY, Gray JL. Numerical modeling of polycristalline CdTe and CIS solar cells. In: Conference record of the twenty third IEEE Photovoltaic Specialists Conference, 1993. p. 586–91.
[5] Gloeckler M, Fahrenbruch AL, Sites JR. Numerical modeling of CIGS and CdTe solar cells: setting the baseline. In: Proceedings of 3rd World Conference on Photovoltaic Energy Conversion, vol. 1, 2003. p. 491–4.
[6] Das C, Du W, Deng X. Modeling of triple junction a-Si solar cells using ASA: analysis of device performance under various failure scenarios. In: Photovoltaic Specialists Conference. Conference Record of the Thirty-first IEEE, 2005. p. 1480–3.
[7] Zeman M, Krc J. Optical and electrical modeling of thin-film silicon solar cells. J Mater Res 2008;23(4):889–98.
[8] Xiao YG, Uehara K, Lestrade M, Li ZQ. Simon Li ZM, Modeling of Si-based thin film triple-junction solar cells. In: Photovoltaic Specialists Conference (PVSC), 34th IEEE, 2009. p. 2154–8.
[9] Merten J, Asensi JM, Voz C, Shah AV, Platz R, Andreu J. Improved equivalent circuit and analytical model for amorphous silicon solar cells and modules. IEEE Trans Electron Devices 1998;45(2):423–9.
[10] Burgelman M, Niemegeers A. Calculation of CIS and CdTe module efficiencies. Sol Energy Mater Sol Cells 1998;51:129–43.
[11] Stutenbaeumer U, Mesfin B. Equivalent model of monocrystalline, polycrystalline and amorphous silicon solar cells. Renewable Energy 1999;18:501–12.
[12] Brecl K, Krc J, Smole F, Topic M. Simulating tandem solar cells. In: Proceedings of 3rd World Conference on Photovoltaic Energy Conversion, vol. 1, 2003. p. 499–502.
[13] Xiao W, Dunford WG, Capel A. A novel modeling method for photovoltaic cells. In: IEEE 35th Annual Power Electronics Specialists Conference, PESC 04, 2004. p. 1950–6.
[14] Burgelman M, Verschraegen J, Degrave S, Nollet P. Modeling thin-film PV devices. Prog Photovoltaics Res Appl 2004;12:143–53.
[15] Werner BA, Prorok M. Analysis of the applicability of the diode equivalent model for GIGS thin-film photovoltaic modules. Photonics and Microsystems. International Students and Young Scientists Workshop; 2006. p. 66–8.
[16] Werner B, Zdanowicz T. Experimental determination of physical parameters in CIGS solar cells. International Students and Young Scientists Workshop on Photonics and Microsystems 2007:84–6.
[17] Ahmad S, Mittal NR, Bhattacharya AB, Singh M. Simulation, output power optimization and comparative study of silicon and thin film solar cell modules. In: 5th IEEE Conference on Industrial Electronics and Applications (ICIEA), 2010. p. 624–9.
[18] Janssen GJM, Slooff LH, Bende EE. 2D - Finite element model of a CIGS module. In: Photovoltaic Specialists Conference (PVSC), 38th IEEE, 2012. 1481–5.
[19] Ishaque K, Salam Z. An improved modelling method to determine the model parameters of photovoltaic (PV) modules using differential evolution (DE). Sol Energy 2011;85:2349–59.
[20] Molina-Garcia A, Bueso MC, Kessler M, Guerrero-Perez J, Fuentes JA, Gomez-Lazaro E. CdTe thin-film solar module modeling using a non–linear regression approach. In: 17th Power Systems Computation Conference, Stockholm, Sweden, August 22–26, 2011.
[21] Ishaque K, Salam Z, Taheri H. Simple, fast and accurate two-diode model for photovoltaic modules. Sol Energy Mater Sol Cells 2011;95:586–94.
[22] Gupta S, Tiwari H, Fozdar M, Chandna V. Development of a two diode model for photovoltaic modules suitable for use in simulation studies. Power and Energy Engineering Conference (APPEEC), Asia-Pacific, 2012. p. 1–4.
[23] Mahmoud YA, Xiao W, Zeineldin HH. A parameterization approach for enhancing PV model accuracy. IEEE Trans Industr Electron 2013;12:5708–16.
[24] Ferdández EF, Siefer G, Almonacid F, García Loureiro AJ, Pérez-Higueras P. A two subcell equivalent solar cell model for III-V triple junction solar cells under spectrum and temperature variations. Sol Energy 2013;92:221–9.
[25] Siddique HAB, Xu P, W. De Doncker R. Parameter extraction algorithm for one-diode model of PV panels based on datasheet values. International Conference on Clean Electrical Power (ICCEP), 2013. p. 7–13.
[26] IEC 60904–3 (Ed. 2), Photovoltaic devices - Part 3: Measurement principles for terrestrial photovoltaic (PV) solar devices with reference spectral irradiance data. 2008.
[27] Shockley W. Electrons and holes in semiconductors. New York: Van Nostrand; 1950.
[28] Yordanov GH, Midtgård O-M. Physically-consistent parameterization in the modeling of solar photovoltaic devices. PowerTech, 2011 IEEE Trondheim; p. 1–4.
[29] Wolf M, Rauscenbach H. Series resistance effects on solar cell measurements. Advanced Energy Conversion 1963;3:455–79.
[30] Markvart T, Costañer L. Solar cells. Materials, manufacture and operation. Elsevier, Oxford, 2005.
[31] <http://www.efn-uk.org/l-street/renewables-lib/solar-reports/index_files/Shell-Solar.pdf>.
[32] Akbaba M, Alattawi MAA. A new model for *I–V* characteristic of solar cell generators and its applications. Sol Energy Mater Sol Cells 1995;37:123–32.
[33] Ortiz-Rivera EI, Peng FZ. Analytical model for a photovoltaic module using the electrical characteristics provided by the manufacturer data sheet. In: Power Electronics Specialists Conference, PESC '05. IEEE 36th 2005. p. 2087–2091.
[34] Massi Pavan A, Castellan S, Quaia S, Roitti S, Sulligoi G. Power electronic conditioning systems for industrial photovoltaic fields: centralized or string inverters? In: International Conference on Clean Electrical Power, ICCEP '07 2007. p. 208–14.
[35] Massi Pavan A, Castellan S, Sulligoi G. An innovative photovoltaic field simulator for hardware-in-the-loop test of power conditioning units. In: International Conference on Clean Electrical Power 2009. p 41–5.
[36] Massi Pavan A, Mellit A, De Pieri D, Lughi V. A study on the mismatch effect due to the use of different photovoltaic modules classes in large-scale solar parks. Prog Photovoltaics Res Appl 2014;22:332–45.
[37] Massi Pavan A, Mellit A, Lughi V. Explicit empirical model for general photovoltaic devices: Experimental validation at maximum power point. Sol Energy 2014;101:105–16.
[38] Karmalkar S, Haneefa S. A physically based explicit J–V model of a solar cell for simple design calculations. IEEE Electron Device Lett 2008;29(5):449–51.
[39] Karmalkar S, Saleem H. The power law J–V model of an illuminated solar cell. Sol Energy Mater Sol Cells 2011;95:1076–84.
[40] Das AK. An explicit J-V model of a solar cell for simple fill factor calculation. Sol Energy 2011;85:1906–9.
[41] Das AK. Analytical expression of the physical parameters of an illuminated solar cell using explicit J–V model. Renewable Energy 2013;52:95–8.
[42] Das AK. An explicit J–V model of a solar cell using equivalent rational function form for simple estimation of maximum power point voltage. Sol Energy 2013;98:400–3.
[43] Saetre TO, Midtgård O, Yordanov GH. A new analytical solar cell *I–V* curve model. Renewable Energy 2011;36:2171–6.
[44] Orioli A, Di Gangi A. A procedure to calculate the five-parameter model of crystalline silicon photovoltaic modules on the basis of the tabular performance data. Appl Energy 2013;102:1160–77.
[45] De Soto W, Klein SA, Beckman WA. Improvement and validation of a model for photovoltaic array performance. Sol Energy 2006;80:78–88.
[46] Villalva MG, Gazoli JR, Filho ER. Comprehensive approach to modeling and simulation of photovoltaic arrays. IEEE Trans Power Electron 2009;24:1198–208.
[47] Lo Brano V, Orioli A, Ciulla G, Di Gangi A. An improved five-parameter model for photovoltaic modules. Sol Energy Mater Sol Cells 2010;94:1358–70.